KfK 5172
Juni 1993

Numerical Study of a 50 kA Current Lead Using Bulk High Temperature Superconductors

R. Heller
Institut für Technische Physik
Projekt Kernfusion

Kernforschungszentrum Karlsruhe

KERNFORSCHUNGSZENTRUM KARLSRUHE

Institut für Technische Physik
Projekt Kernfusion

KfK 5172

NUMERICAL STUDY OF A 50 KA CURRENT LEAD USING BULK HIGH TEMPERATURE SUPERCONDUCTORS

R. Heller

Kernforschungszentrum Karlsruhe GmbH, Karlsruhe

Als Manuskript gedruckt

Kernforschungszentrum Karlsruhe GmbH
Postfach 3640, 7500 Karlsruhe 1

ISSN 0303-4003

Abstract

Based on the design of the 30 kA current lead with a low temperature superconductor (LTSC) forseen for the test of a superconducting pulsed model coil (POLO model coil) in the test facility TOSKA at KfK, a 50 kA current lead for the future test of a model coil for the International Thermonuclear Experimental Reactor ITER in the TOSKA facility was proposed resulting in a helium mass flow rate normalized to the current of 0.055 g/(s-kA) at 50 kA resp. of 0.015 g/(s-kA) at zero current.

In this paper, the possibility of the use of High Temperature Superconductors (HTSC) for high current carrying current leads cooled by forced flow supercritical helium has been investigated in order to study the capabilities.

The current lead behaviour has been theoretically studied under different conditons: zero current operation, nominal current (50 kA) operation, extended current (70 kA) operation, and safety behaviour (loss of helium mass flow). Two design cases which differ in the current sharing and critical temperatures of the HTSC have been investigated in order to look on the amount of helium mass flow reduction.

The result is that the reduction of mass flow rate will be 50 % at zero current and about 10 to 20 % at 50 kA for the two cases. The transient behaviour of the HTSC lead differs considerably from the one of the LTSC lead due to the high electrical resisitivity of the HTSC.

Numerische Studie einer 50 kA Stromzuführung unter Verwendung von Bulk-Hochtemperatur-Supraleitern

Zusammenfassung

Aufbauend auf dem Design der 30 kA Stromzuführung mit einem Einsatz bestehend aus herkömlichem Supraleiter, welche für den den Test der POLO Modellspule vorgesehen ist, wurde eine Stromzuführung für 50 kA vorgeschlagen, die für den Test einer Modellspule für ITER verwendet werden kann. Der Massenstrom bezogen auf den Betriebsstrom beträgt danach 0.055 g/(s-kA) bei 50 kA bzw. 0.015 g/(s-kA) bei Nullstrom.

In diesem Bericht wurde die Möglichkeit der Verwendung von Hochtemperatursupraleitern in einer zwangsgekühlten Hochstromzuführung untersucht.

Die Eigenschaften dieser Stromzuführung wurden unter veschiedenen Bedinungen theroretisch untersucht: Nullstrombetrieb, Nominalbetrieb (50 kA), Überstrombetrieb (70 kA) und Sicherheitsmarge bei Massenstromausfall. Zwei Fälle, die sich in der kritischen Temperatur des Hochtemperatursupraleiters unterscheiden, wurden untersucht in Hinblick auf die Reduzierung des Heliummassenstroms, verglichen mit einer herkömlichen Stromzuführung.

Das Ergebnis ist, daß die Reduzierung des Massenstroms im Nullstrom Fall 50 Prozent und bei 50 kA 10 bis 20 Prozent beträgt. Das transiente Verhalten einer Hochtemperatur-Stromzuführung unterscheidet sich beträchtlich von einer vom POLO-Typ infolge des hohen elektrischen Widerstands des Hochtemperatursupraleiters im normalleitenden Zustand.

Contents

1.0 Introduction **1**
1.1 Motivation 1
1.2 Short overview about existing HTSC current leads 2
1.3 Material properties 3

2.0 Results of steady state calculations **7**
2.1 Optimization of current lead lengths 7
2.2 Nominal operation 11
2.3 Stand-by operation 12
2.4 Extended (70-kA-)operation 13
2.5 Steady-state load line of the current lead 15

3.0 Loss of helium mass flow **22**

4.0 Summary and conclusions **29**

5.0 References **33**

Figures

1. Schematic view of the copper and the HTSC current lead 2
2. Heat capacity of YBCO and comparison to pure copper 3
3. Thermal conductivity λ of YBCO resp. BSCCO and comparison to copper 4
4. Critical current density vs applied magnetic field of BSCCO and YBCO 5
5. Helium mass flow rate vs conductor length 8
6. Temperature profiles vs conductor length for a copper and a HTSC current lead for two different mass flow rates each 10
7. Heat leakage towards the low temperature end of a copper and a HTSC current lead vs helium mass flow rate normalized to the minimized mass flow rate 11
8. Temperature profile of the HTSC current lead at 50 kA and comparison to the copper lead 12
9. Temperature profile of the HTSC current lead at 0 kA and comparison to the copper lead 13
10. Temperature profile of the HTSC current lead at 70 kA and comparison to the copper lead 14
11. Temperature profiles of the HTSC current lead (case I) for different currents 16
12. Minimized helium mass flow rate vs current for the HTSC current lead and comparison to the copper lead 17
13. Temperature at the upper end of the HTSC conductor of the current lead vs current . 18
14. Voltage drop of the current lead vs current 19
15. Reduction factor r in % vs current of the HTSC leads and comparison to the copper lead 20
16. Temperature profile of the HTSC lead (case I) vs position in case of loss of mass flow at 50 kA 23
17. Temperature profile of the HTSC lead (case II) vs position in case of loss of mass flow at 50 kA 24
18. Temperature profile of the copper lead vs position in case of loss of mass flow at 50 kA 25
19. Maximum temperature in the HTSC part of the HTSC leads vs time in case of loss of mass flow at 50 kA 26
20. Voltage drop along the current lead vs time of the HTSC leads and the copper lead in case of loss of mass flow at 50 kA 27
21. Heat leakage at the low temperature end of the HTSC leads and the copper lead vs voltage drop in case of loss of mass flow at 50 kA 28
22. Schematic view of the 50 kA-HTSC-current lead 31

Tables

1. Characterization of the copper and HTSC leads in terms of electrical resistivity ρ and thermal conductivity λ 2
2. Input parameters of the heat exchanger for the proposed HTSC current lead 9
3. Main results of the load line calculations for the POLO-type copper and and for the HTSC leads of cases I and II 21
4. Geometrical quantities of the heat exchanger of the HTSC current lead 30
5. Helium mass flow rates normalized to the current at 0 kA and 50 kA for the HTSC leads and the copper lead 32
6. Cryogenic load of the HTSC leads and comparison to the copper lead for the ITER model coil test in TOSKA 32

1.0 Introduction

1.1 Motivation

In [1], the design of a 50 kA current lead made of phosphorous deoxidized copper and adding Nb_3Sn insertions in the lower temperature part of the lead for getting minimum losses in a wide current range has been presented for the ITER model coil test in TOSKA-Upgrade. The design is an extrapolation of the 30 kA / 23 kV current lead developed and tested at the Institut für Technische Physik for the POLO model coil test in TOSKA. [2]. The reason of using Nb_3Sn inserts was not **the reduction of the thermal load** but **the minimization of the helium mass flow rate in a wide current range**.

The specifications of the TOSKA-Upgrade facility has been given in [3]. The power margin available for heat load tests, i.e. simulations of the AC losses during plasma disruption, divertor sweeping, coil charge and discharge, as well as simulation of nuclear heating will be about 300 W.

Because the main origin of the static load to the refrigerator power are the current leads, it would be useful to search for possibilites for further reductions. This can not be done by further optimization of conventional copper leads because here the physical limit for the specific mass flow rate of 0.05 g/(s-kA) has practically been reached in the POLO lead design. Therefore other design paths have to be opened as:

- stepwise reduction of the conductor cross section towards the low temperature end [4], [5],
- use of superconductors with or without copper in parallel [7], [8],
- use of a low thermal conductivity material, e.g. brass, and
- use of high temperature superconductors.

In this report, the latter possibility will be studied.

Figure 1 shows a scheme of a copper current lead including Nb_3Sn inserts in the low temperature part (POLO type lead) resp. the HTSC current lead:

- Copper lead:
  It consists of a room temperature region which carrys the connections to the power supply, a heat exchanger region, i.e. central copper conductor surrounded by perrforated copper disks, and a low temperature heat exchanger region of the same type including Nb_3Sn superconductor inserts.
- HTSC lead:
  It consists of a room temperature region which carrys the connections to the power supply, a heat exchanger region, i.e. central copper conductor surrounded by perrforated copper disks, and a low temperature region made of HTSC superconductor.

The figure illustrates the main difference of the two approaches. Table 1 summarizes the main properties of the two schemes.

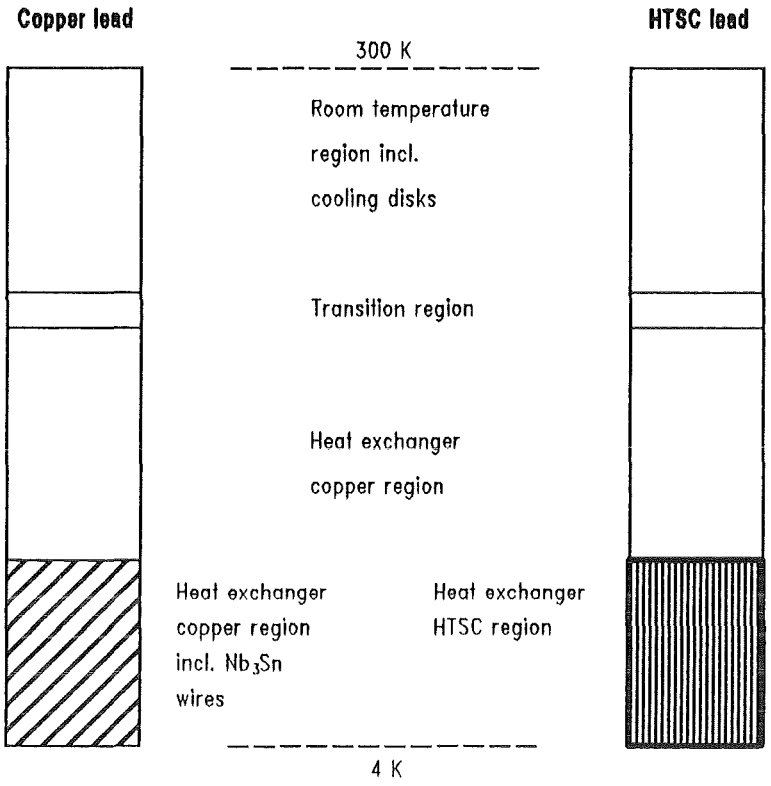

Figure 1. Schematic view of the copper and the HTSC current lead

Region	Joule heating		Heat conduction	
	Copper lead	HTSC lead	Copper lead	HTSC lead
Low temperature heat exchanger	0 for $T < T_c$ $\rho_{Cu,RRR=5} \cdot I^2$ for $T \geq T_c$	0 for $T < T_c$ $\rho_{HTSC} \cdot I^2$ for $T \geq T_c$	$\lambda_{Cu,RRR=5}$	λ_{HTSC}
Heat exchanger	$\rho_{Cu,RRR=5} \cdot I^2$	$\rho_{Cu,RRR=5} \cdot I^2$	$\lambda_{Cu,RRR=5}$	$\lambda_{Cu,RRR=5}$
Transition region	$\rho_{Cu,RRR=5} \cdot I^2$	$\rho_{Cu,RRR=5} \cdot I^2$	$\lambda_{Cu,RRR=5}$	$\lambda_{Cu,RRR=5}$
Room temperature end	$\rho_{Cu,RRR=5} \cdot I^2$	$\rho_{Cu,RRR=5} \cdot I^2$	$\lambda_{Cu,RRR=5}$	$\lambda_{Cu,RRR=5}$

Table 1. Characterization of the copper and HTSC leads in terms of electrical resistivity ρ and thermal conductivity λ. RRR is the residual resistivity ratio, i.e. ρ(273 K)/ ρ(4 K)

1.2 Short overview about existing HTSC current leads

In literature, a large number of papers is present in which the use of high temperature superconductor as a conductor for current leads is described ([9] - [19]). Several papers present results of design studies, others describe design and test results of prototypes operating in a current range of 1 - 2 kA. Existing designs can be divided into several classes:

- Type of superconductor used in the lower temperature part (4 K - 77 K), e.g.

1. $YBa_2Cu_3O_7$ (YBCO) without and with admixture of silver of different amount, having a T_c = 92 K,
2. $Bi_{2-x}Pb_xSr_2Ca_2Cu_3O_x$, having a T_c = 110 K, and $Bi_2Sr_2Ca_2Cu_2O_x$, having a T_c = 80 K, (BSCCO)

- Cooling mode, i.e.
  1. Liquid helium cooling from 4 K to room temperature,
  2. No cooling up to 77 K and liquid nitrogen (LN_2) cooling from 77 K to room temperature, and
  3. Combined cooling, liquid helium from 4 K to 77 K and nitrogen from 77 K to room temperature.

The reported reduction of heat leakage is in the order of 30 - 60 % depending on the operational current and the design.

1.3 Material properties

Figure 2 shows the heat capacity of a YBCO HTSC as given in [21]. For comparison, the heat capacity of pure copper has been added. This shows that the heat capacity of both materials are very similar.

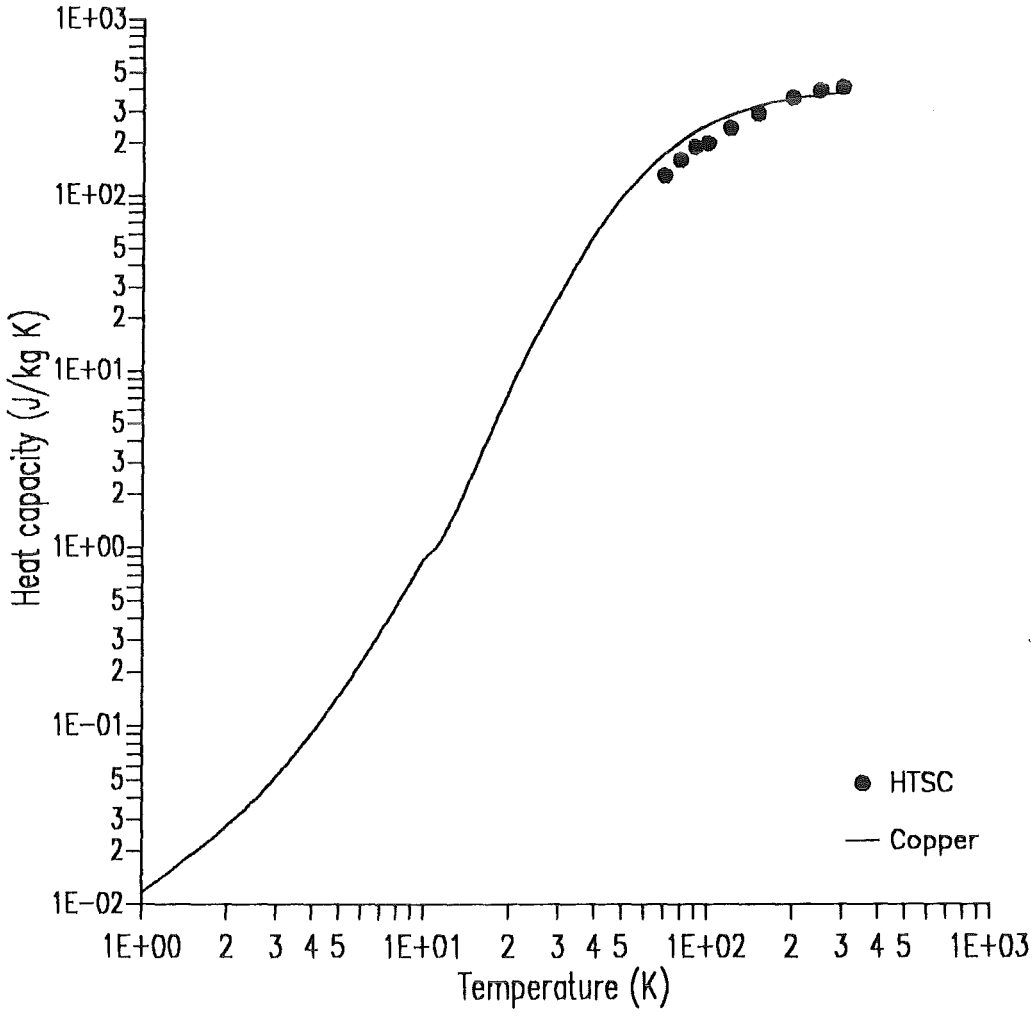

Figure 2. Heat capacity of YBCO and comparison to pure copper. The full circles are measurement data from [21] whereas the full line corresponds to a fitted spline to copper data

In Figure 3, the thermal conductivities of pure sintered YBCO (dash-dotted line, fitted data as given in [9]), and sintered YBCO with 10 wt.% silver content (full line, cubic spline to data given

in [15]) are plotted. The thermal conductivity data of BSCCO are given, too, i.e. Bi-2212 data as a dashed line, and Bi-2223 data as a long-dashed line, both data are presented in [16]. For comparison, the thermal conductivities of copper with different residual resistivity ratios (RRR) are shown as well as measurement data of phosphorous deoxidized copper (RRR=5) used for the POLO current lead (full circles).

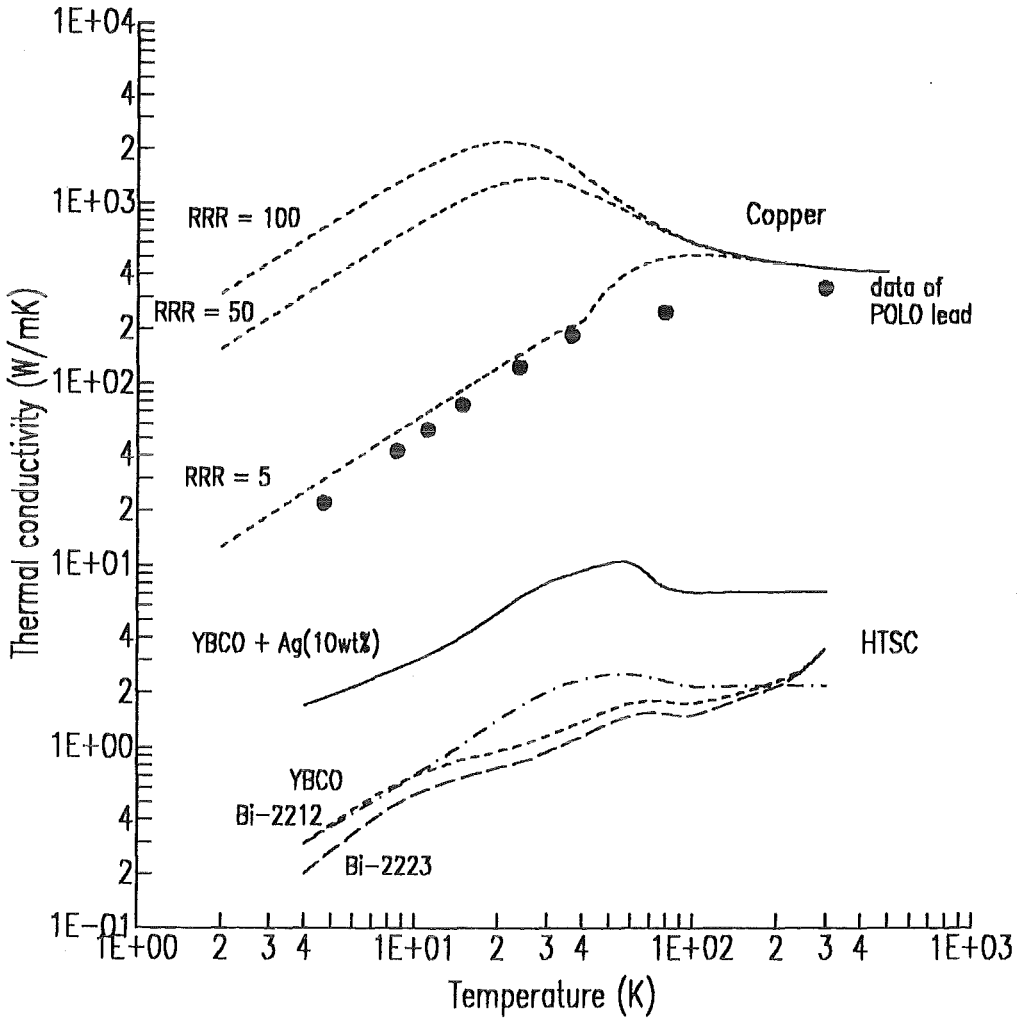

Figure 3. Thermal conductivity λ of YBCO resp. BSCCO and comparison to copper. The full line corresponds to data from silver doped YBCO measured by [15], the dash-dotted line represents fitted data used in [9], the dashed line corresponds to Bi-2212 data given in [16], the long-dashed line respresents Bi-2223 data from [16], the full circles are measurement data of copper used in the POLO current lead, the dashed lines correspond to fitted splines of copper data of different RRR

The very low thermal conductivity of the HTSC material is the main reason for looking on the possibility for using it as a conductor for current leads. Nevertheless, the thermal conductivity depends strongly on the quality of the material (see e.g. [16]).

In Figure 4, the critical current densities of YBCO resp. BSCCO superconductors at 77 K are plotted as a function of the applied magnetic field as presented in [16] (field orientation perpendiculra and parallel to current flow direction) resp. [20] (field orientation perpendicular to current flow direction). The well known strong decrease of the critical current density with increasing magnetic field resp. orientation of the applied magnetic field is clearly seen as well as the wide range of critical current density depending on the size of the superconductor resp. the preparation, e.g. with or without silver contents etc.

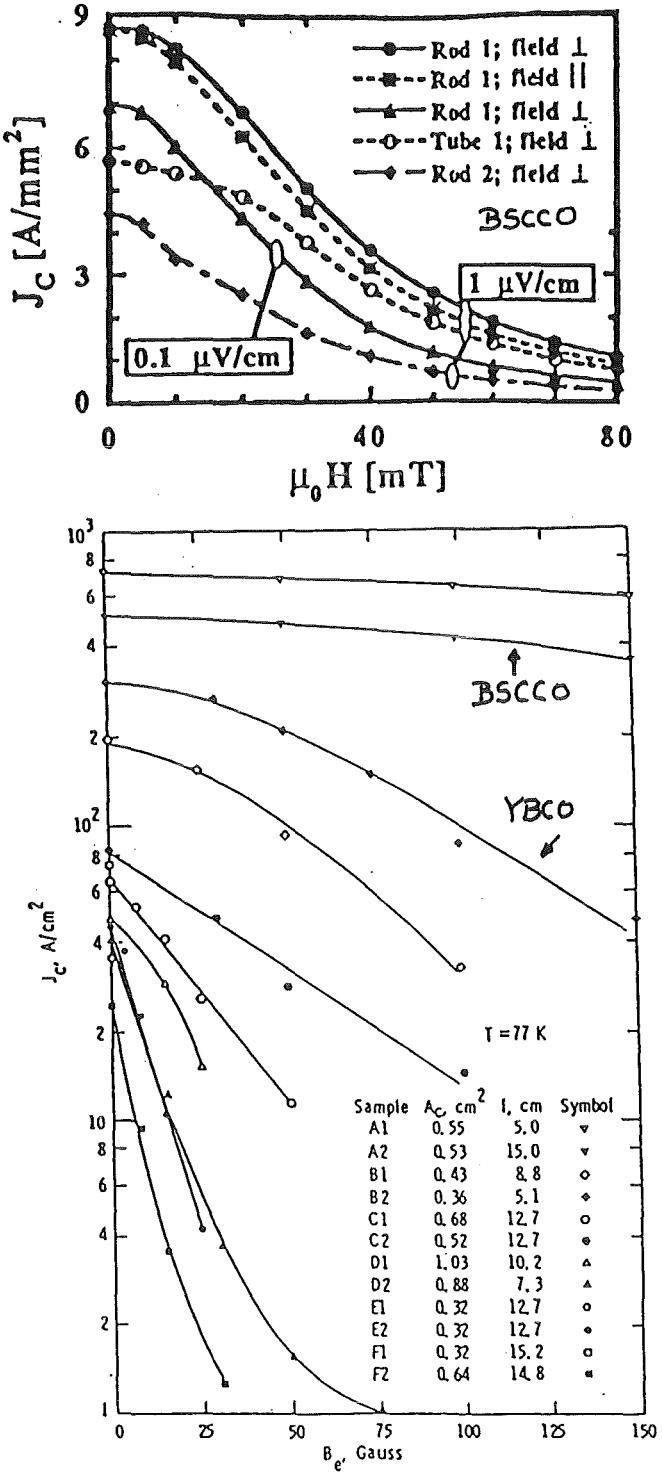

Figure 4. Critical current density vs applied magnetic field of BSCCO and YBCO. The data shown on top are taken from [16] the ones shown on bottom are given in [20] (1 Gauss = 0.1 mT)

Summing up the material properties of the HTSC, the critical issues of any HTSC design are:

1. Thermal conductivity:
   The low thermal conductivity of the HTSC materials results in a large electrical resistivity in the normal conducting case. In [9], the Lorentz number of YBCO is given to be $L_0 = 3.16 \cdot 10^{-8} W\,\Omega / K^2$ whereas for pure metals, $L_0 = 2.45 \cdot 10^{-8}\ W\,\Omega / K^2$, i.e. about 25 % lower. Therefore, the electrical resistivity of YBCO would be about two orders of magnitude higher than for copper.
2. Critical current density at 77 K in externally applied magnetic fields as well as in self-fields:

A lead carrying currents of up to 70 kA produces a self-field which will be in the order of 0.1 to 0.4 T depending on the cross section. To this number the background field of the magnetic device, i.e the superconducting coil, has to be added vectorially to get the total applied field. In case of the ITER model coil test, large background field in the current lead region up to 2.5 T are expected [22]. It is well known that the critical current of the HTSC depends strongly on the direction of the applied magnetic field with respect to the current flow axis.

3. Brittleness of the HTSC materials:
   For mechanical stability reasons, addition of silver to the HTSC is favoured. This increases the thermal conductivity of the material depending on the amount of silver admixture. In addition, the addition of silver also affects the critical current density.
4. Dimension of HTSC conductors:
   For technical and electromagnetic stability reasons, e.g. manufacturing of HTSC rods with cross sections and lengths needed for current lead application, AC losses, cooling etc., the conductor of the HTSC part has to be subdivided in the cross sectional area. Due to manufacturing problems, this influences strongly the height of the critical current as well as its dependence on applied magnetic field.

These requirements lead to the following boundary conditions of the design:

- The HTSC cross-sections will be considerably larger compared to copper. Looking on Figure 3, the difference in thermal conductivity between YBCO / BSCCO and phosphorous deoxidized copper is about one to two orders of magnitude. Assuming a critical current density of HTSC of 2.5 A/mm² at 77 K and a magnetic field of 0.1 T, and an operation current density in copper of 15.6 A/mm², the ratio of the current density is about one order of magnitude. Besides space problems the advantage of low thermal conductivity is partly cancelled by the low operation current density at 77 K in high magnetic fields.
- This problem mentioned could be much reduced if the temperature at the upper end of the HTSC part will be (much) below 77 K, e.g. 20 K. The reduction of thermal load of a HTSC current lead working at an upper temperature of 20 K will be less than for a lead working at 77 K.
- Due to the large electrical resistivity in normal state operation, the cross section of the HTSC conductor should be anyhow large to increase the burn-out-time in case of loss of coolant.
- Due to the large cross section of HTSC materials, AC losses during transient current operation have to be taken into account, too.

Despite these limitations, a HTSC current lead will be described in the following sections being able to carry current densities of 4 A/mm² above 77 K. Alternatively, a second approach will be presented working at a lower temperature level at the upper end of the HTSC part.

2.0 Results of steady state calculations

In the following, design criteria are presented based on a 50 kA copper current lead for the ITER Model coil test in TOSKA. YBCO high temperature superconductors will be used in the low temperature part for the optimization procedure.

The calculations were done by means of the computer code CURLEAD [23] and [24], which was extended to the use of YBCO-HTSC material. The thermal conductivity given by [15] is used, the electrical resistivity in the normal conducting case is calculated by means of the Lorentz number given in [15], and the heat capacity is taken by fitting a cubic spline to data points given in [21] resp. by a cubic extrapolation to the low-temperature-region.

2.1 Optimization of current lead lengths

At 50 kA, i.e. nominal operation current, the length of the copper conductor for a fixed length of the HTSC conductor has been varied to find the minimum mass flow rate. This was done for two different current sharing resp. critical temperature levels, i.e.

1. 82 K / 95 K - **case I** resp.
2. 20 K / 30 K - **case II**.

The current sharing resp. critical temperatures have been defined such that

$$I_c(T = T_{cs}) / I_{op} = 1,$$
$$I_c(T = T_c) / I_{op} = 0.$$

The increase of the electrical resistivity is linear between the current sharing and the critical temperature.

After that, the same procedure has been done for the HTSC conductor. In Figure 5, the mass flow rate through the current lead is plotted vs the copper resp. HTSC conductor lengths. The result is the following:

1. Copper conductor:
   For conductor lengths smaller than the optimum one, the mass flow rate is determined by the heat leakage at the lower end of the lead. A heat leakage of 1 W was arbitrarily chosen as limitation.

   For conductor lengths larger than the optimum one, the mass flow rate is determined by the temperature at the warm end of the conductor.
2. HTSC conductor:
   For conductor lengths smaller than the optimum one, the mass flow rate is determined by the heat leakage at the lower end of the lead. As for the length optimization of the copper part a heat leakage of 0.7 W was chosen as limitation too.

   For conductor lengths larger than the optimum one, the minimized mass flow rate is independent of the length because no Joule heat production takes place at the warm end of the HTSC part.

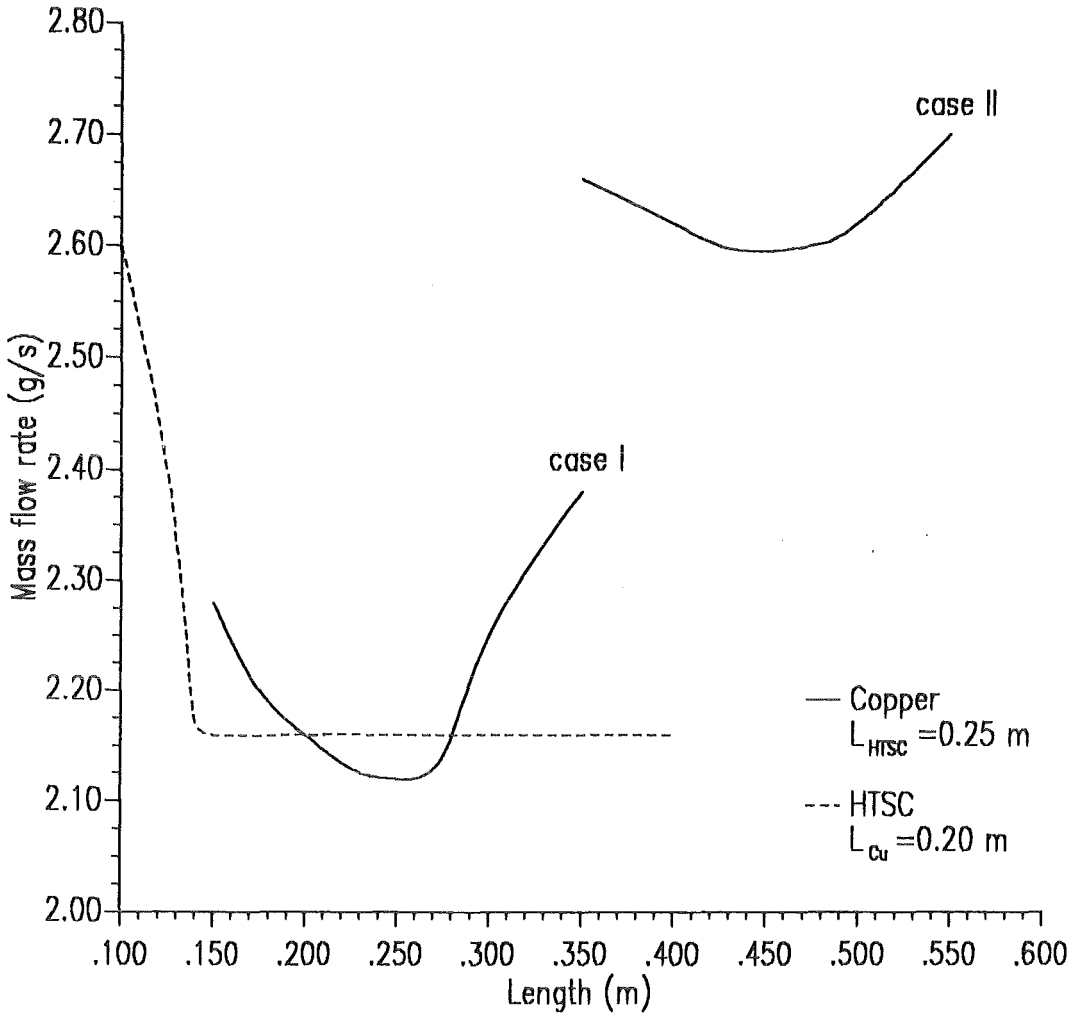

Figure 5. Helium mass flow rate vs conductor length. The dashed line corresponds to the HTSC, the full line corresponds to the copper conductor using two different current sharing / critical temperature sets for the HTSC.

As a conclusion of the calculations, the length of the HTSC conductor was set to 0.25 m. The length of the copper conductor was set to 0.20 m (case I), i.e. smaller than the optimum length to have lower mass flow rates at higher current, resp. to 0.45 m (case II).

Table 2 summarizes the geometrical parameters of the current lead. The parameters of the cooling disks of the copper heat exchanger as well as of the copper conductor are slightly different to the ones given in [1].

Parameter	Unit	Value	
		HTSC part	Copper part
Heat exchanger type		rectangular rods parallel orientated	central conductor surrounded by perforated copper plates
Length	m	0.25	0.20 (case I) 0.45 (case II)
Cross section of conductor A_{Cu}	cm^2	174.0	38.5
Cooled perimeter of heat exchanger P_{cool}	m	10.44	11.77
Cross section of helium A_{He}	cm^2	159.0	3.86
RRR of cooling disks			50
Rib efficiency of cooling disks		n.a.	function of temperature
Cross sectional dimensions of HTSC rod	mm x mm	10 x 5	
Number of HTSC rods		348	
Total length of lead	m	0.72 (case I) 0.97 (case II)	
Helium inlet temperature	K	4.50	
Helium inlet pressure	MPa	0.40	
Conductor temperature at low-temperature end	K	4.50	
Conductor temperature at upper end of HTSC part	K	< 82 (case I) < 20 (case II)	
Conductor temperature at high-temperature end	K	295	

Table 2. Input parameters of the heat exchanger for the proposed HTSC current lead. n.a. = not available

During the optimization procedure, an interesting result has been obtained which relates to a fundamental distinction between a copper and a HTSC current lead concerning burn-out conditions:

1. For the HTSC lead the burn-out region will be localized, i.e. slightly below the upper end of the HTSC part because the electrical resistance of the HTSC is about two orders of magnitude larger than for copper. A consequence is that the increase of the heat leakage towards the low temperature end of the lead is less sharp if the mass flow rate is reduced below the minimized one.
2. For the copper lead the burn-out region will be more distributed around 80 per cents in heat exchanger length and the heat leakage towards the low temperature end of the lead rises sharply if the mass flow rate is reduced below the minimized one.

This is clearly seen in Figure 6 where the temperature profile as a function of position is plotted for a copper lead and a HTSC/copper lead for two different helium mass flow rates each, one being below and one being above the minimized mass flow rate. Figure 7 shows the heat leakage towards the low temperature end of the lead as a function of the helium mass flow rate normalized to the minimized mass flow rate, once for the HTSC lead (full line) and once for the copper lead (dashed line).

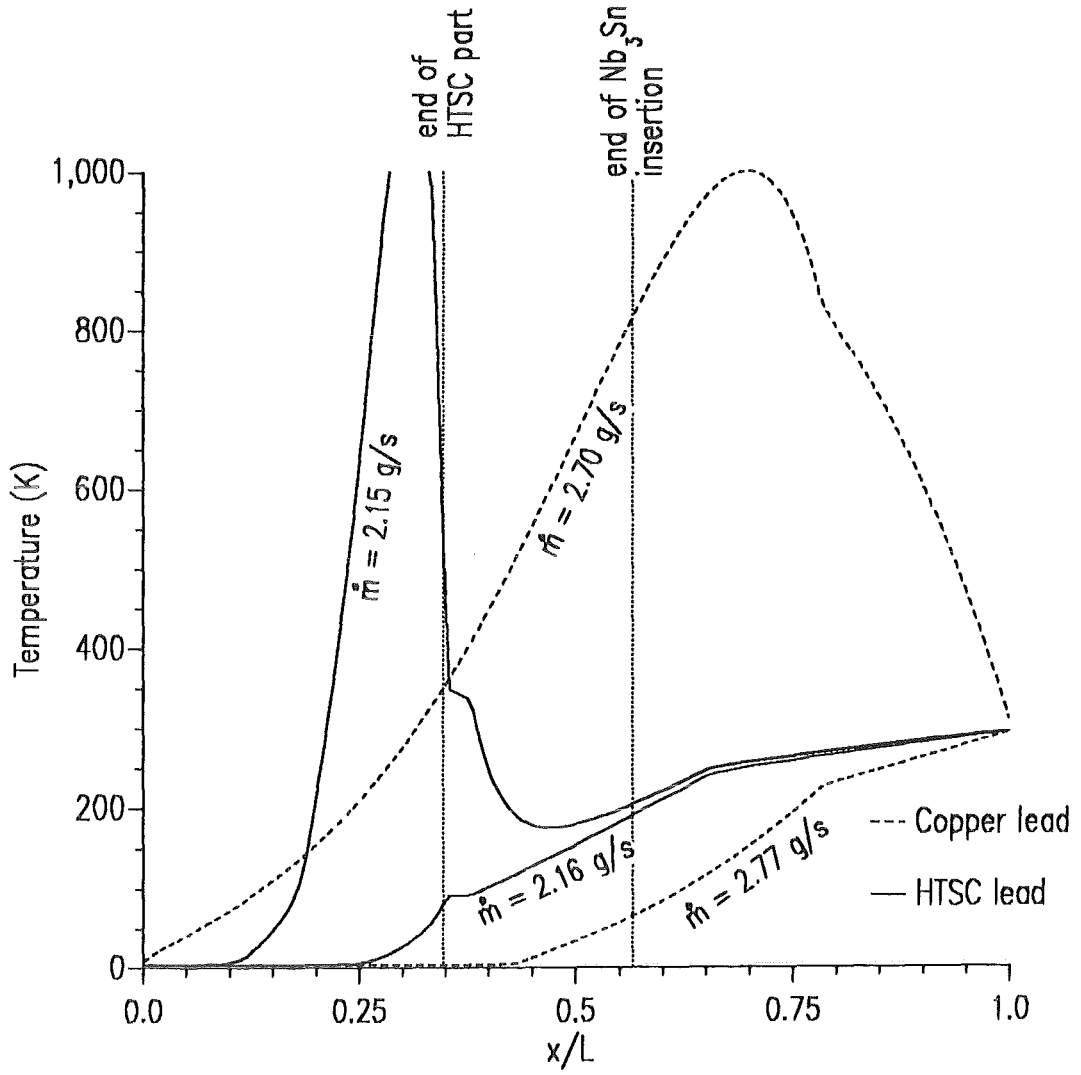

Figure 6. Temperature profiles vs conductor length for a copper and a HTSC current lead for two different mass flow rates each. The full lines correspond to the HTSC lead the dashed lines to the copper lead

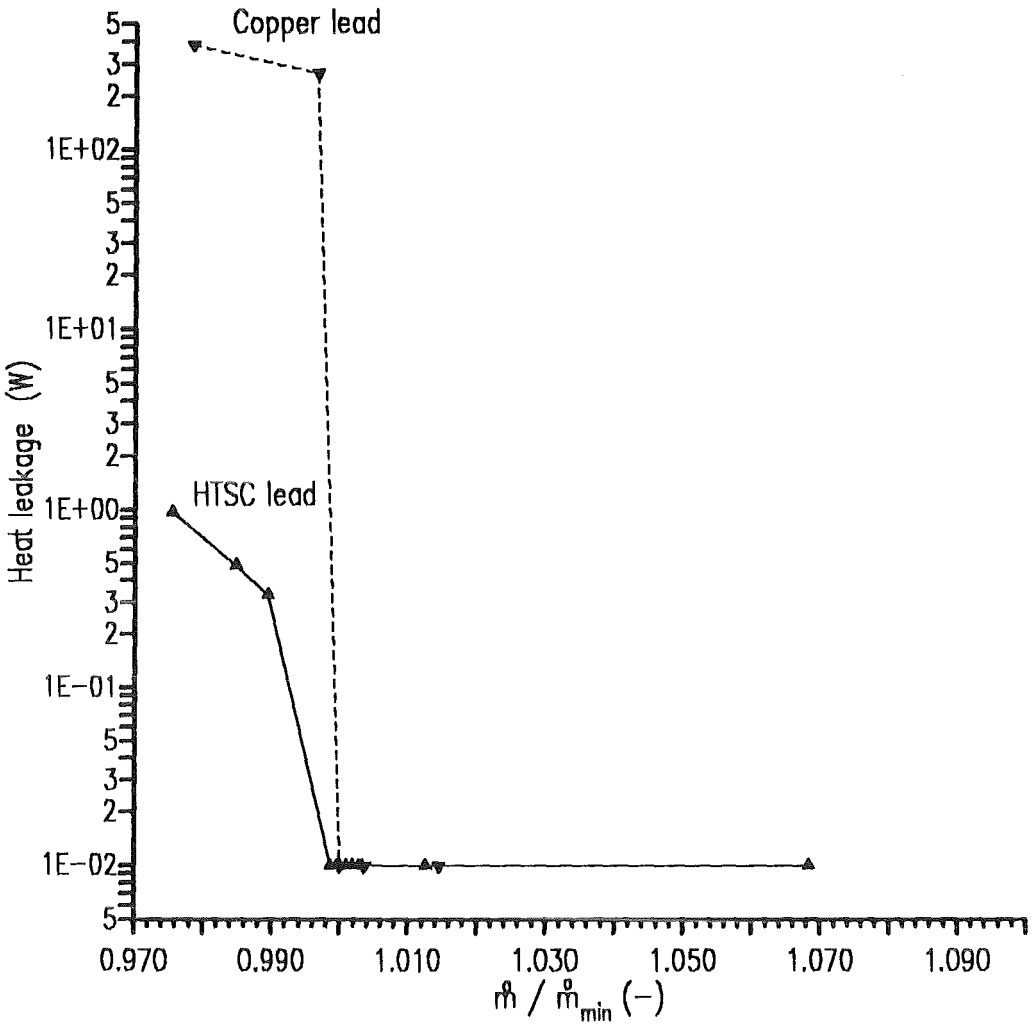

Figure 7. Heat leakage towards the low temperature end of a copper and a HTSC current lead vs helium mass flow rate normalized to the minimized mass flow rate. The full lines correspond to the HTSC lead the dashed lines to the copper lead

In the next sections, the results of the calculations for currents up to 70 kA are presented and compared to the ones for a POLO-type current lead, i.e. a copper conductor with Nb_3Sn insertions to get minimum mass flow rates for different currents and for zero current ("stand-by-mode").

2.2 *Nominal operation*

The temperature profiles of the optimized current leads are shown in Figure 8 whereas the numbers are given in Table 3 at the end of this chapter.

Although the total length of the HTSC lead of case I is much smaller than for the copper lead (0.72 m instead of 1.15 m), the minimized mass flow rate is only 2.16 g/s (HTSC lead) instead of 2.77 g/s (copper lead). The reason is the low thermal conductivity and the high critical temperature of the HTSC material resulting in a high temperature at the lower end of the copper part. For case II, the minimized mass flow rate is 2.60 g/s, i.e. much higher than for case I. The reason is the lower critical temperature resulting in a longer length of the copper conductor.

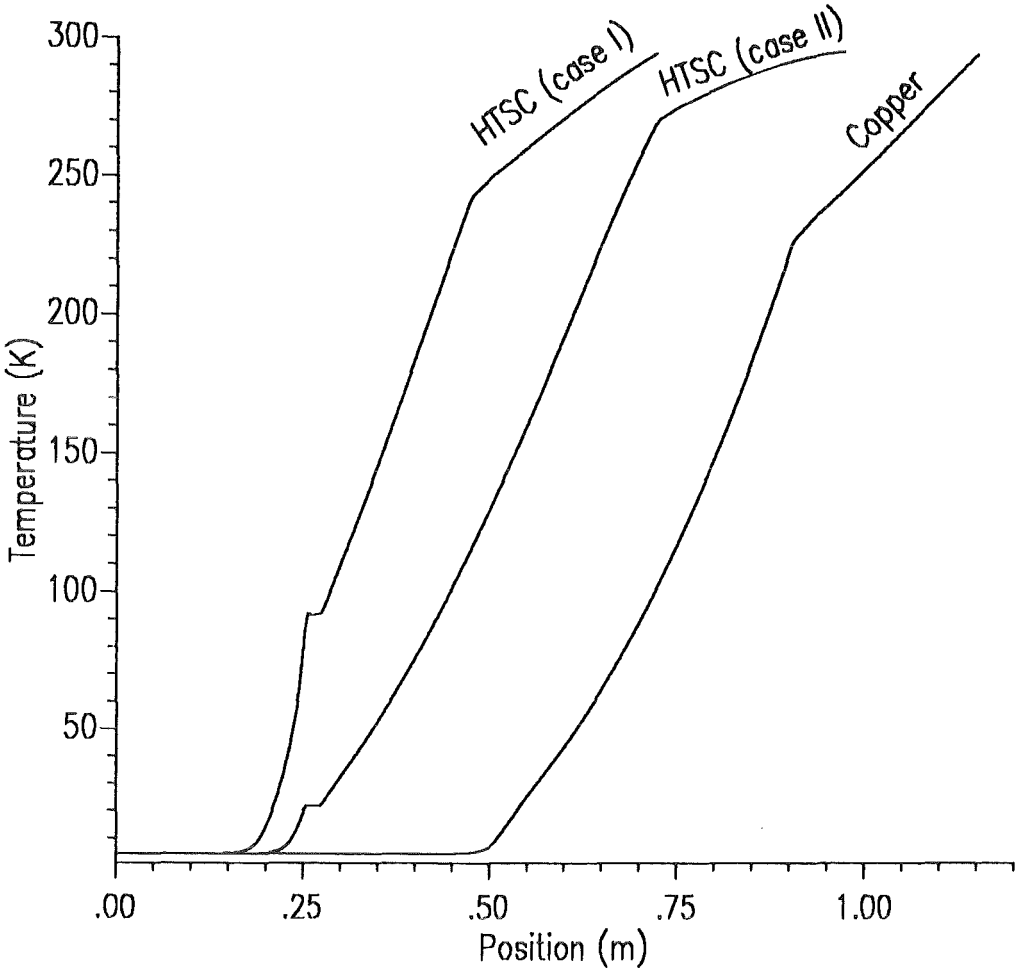

Figure 8. Temperature profile of the HTSC current lead at 50 kA and comparison to the copper lead

2.3 *Stand-by operation*

The temperature distributions for zero current ("stand-by") have been computed, too. The criterion of the minimization procedure of the mass flow rate was the aim to get a heat leakage at the low temperature end of the lead of about 0.8 W.

Figure 9 shows the temperature profiles for the HTSC leads (case I and II) resp. the copper lead for comparison. In Table 3 at the end of this chapter, the numbers are given.

The minimized mass flow rate of the HTSC lead is 0.45 g/s in case I resp. 0.40 g/s in case II whereas the POLO-type copper lead needs a mass flow rate of 0.85 g/s. Also here, the reason is the low thermal conductivity of the HTSC material resulting in a high temperature at the upper end of the HTSC part. This will be discussed later.

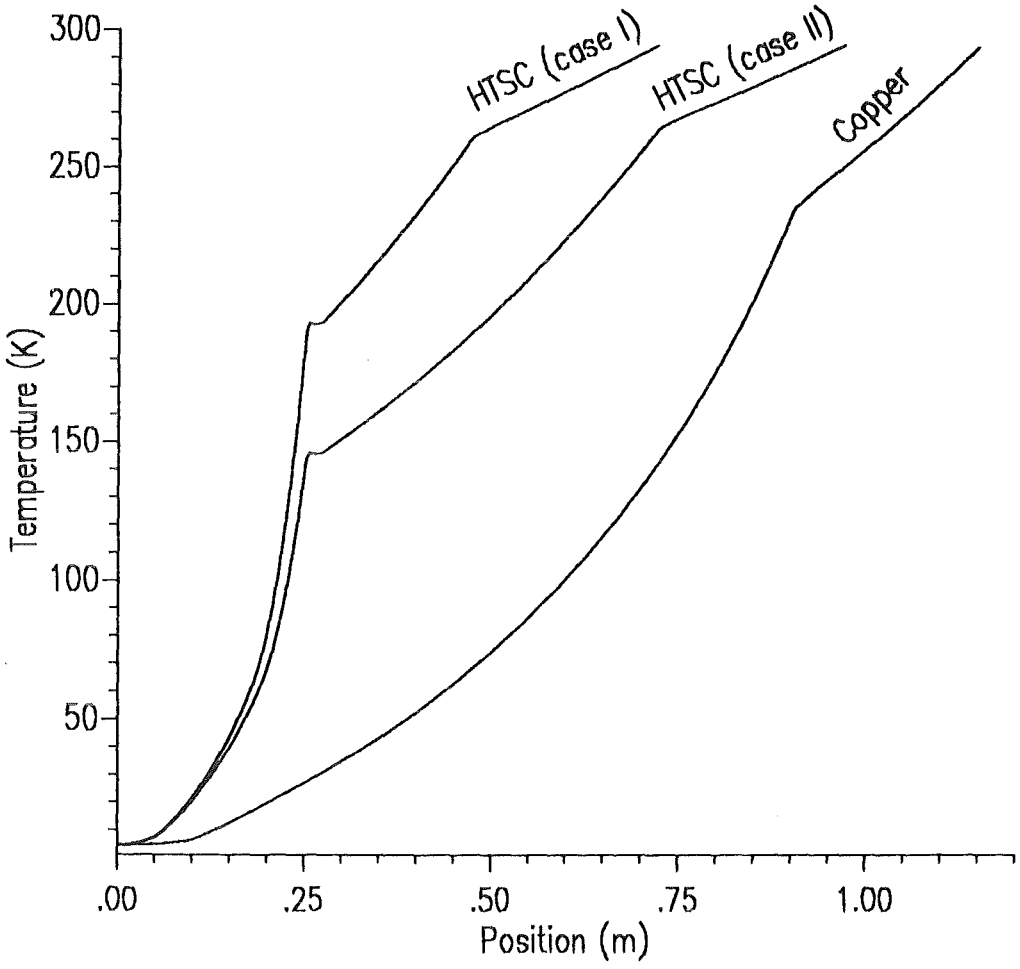

Figure 9. Temperature profile of the HTSC current lead at 0 kA and comparison to the copper lead

2.4 Extended (70-kA-)operation

The design of the current leads was made in view of the boundary condition to carry a maximum current of 70 kA in a stable manner. Because the optimization was done for 50 kA, the helium mass flow rates at 70 kA are no longer optimized ones neither the copper lead nor the HTSC leads of cases I and II. But it would be possible to operate the leads at 70 kA at steady state conditions.

Figure 10 shows the temperature profiles of the HTSC leads of case I, of case II, and of the copper lead for comparison. All temperature profiles are based on minimized mass flow rates. The corresponding numbers are summarized in Table 3 at the end of this chapter.

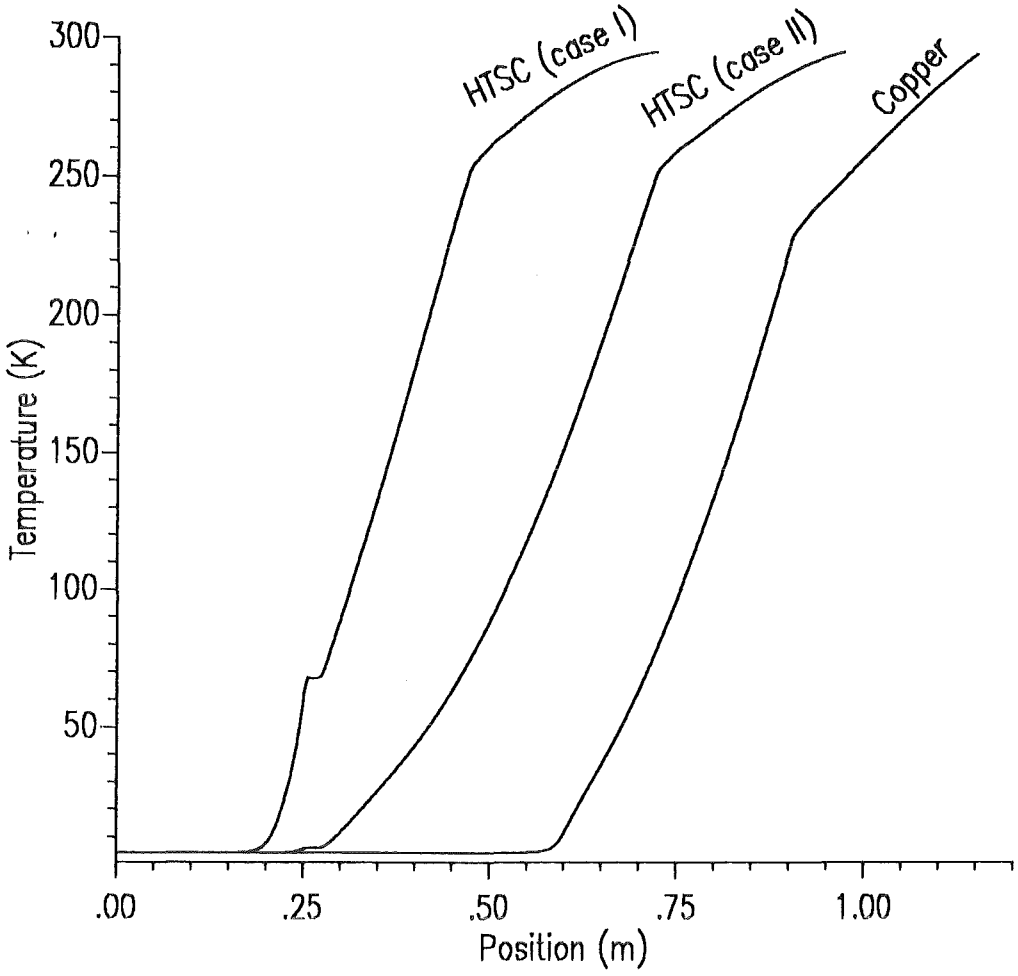

Figure 10. Temperature profile of the HTSC current lead at 70 kA and comparison to the copper lead

The minimized mass flow rates for the HTSC leads are 3.20 g/s (case I) resp. 4.40 g/s (case II) whereas for the POLO-type lead the helium mass flow rate is 3.85 g/s, i.e in between. The reason is that due to the longer length of the copper part of the HTSC lead of case I, the Joule heat production is much higher than for case I resulting in a higher mass flow rate needed for cooling.

2.5 *Steady-state load line of the current lead*

The steady state load line of the current leads was calculated by minimizing the helium mass flow rate for 0 to 70 kA in steps of 5 to 10 kA thus to get minimum losses at the low temperature end and no overheating at the warm end. This has been done for cases I and II and for comparison for the POLO type copper lead, too.

Figure 11 shows the temperature profiles for the HTSC lead of case I for different operating currents. The upper end of the HTSC part of the lead is clearly seen as a step in the temperature profile indicating the transition region between the HTSC and the copper conductor. For currents below 30 kA (here called transition current), the temperature at the upper end of the HTSC part is above the critical temperature, i.e. the Joule heating in the HTSC conductor can be transferred to the helium. For currents of 30 kA and above, the helium is no longer able to transport the heat produced in the HTSC conductor being in the normal conducting phase. Therefore, the temperature in the HTSC has to be below the critical temperature at any location to prevent Joule heat.

The HTSC lead of case II shows the same behaviour, the transition current is now 20 kA.

It should be noted here, that the effect of small heat production in the HTSC, if working near the critical current, has not been studied here. Only heat conducting, heat production, and heat transfer has been taken into account.

In Figure 12, the minimized helium mass flow rate is plotted as a function of the current for both HTSC leads and also for the copper lead. Here the effect of the temperature at the upper end of the HTSC conductor part is also seen: The "wiggle" in the curve around the transition current is also due to the change in the temperature at the upper end of the HTSC conductor. The latter one is plotted in Figure 13 whereas in Figure 14 the voltage drop along the lead conductor is plotted as a function of current for the HTSC leads of cases I and II, and of the copper lead.

Figure 15 shows the reduction factor of the helium mass flow rates for the HTSC leads of cases I and II compared to the POLO-type copper lead. The reduction factor r [%] is defined as follows:

$$r = \frac{\dot{m}_{HTSC} - \dot{m}_{Cu}}{\dot{m}_{Cu}} \cdot 100$$

where
$\dot{m}_{HTSC}$ = mass flow rate of HTSC lead, and
$\dot{m}_{Cu}$ = mass flow rate of Copper lead.

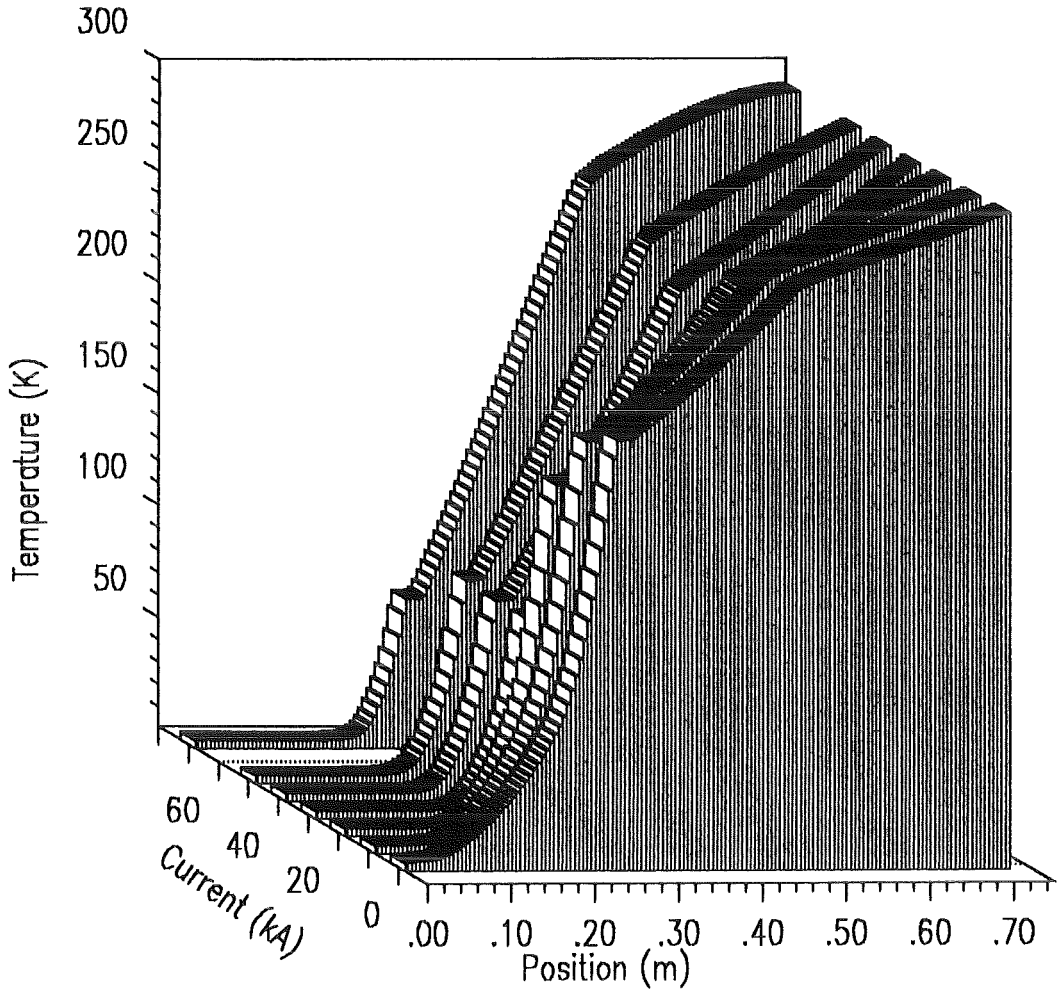

Figure 11. Temperature profiles of the HTSC current lead (case I) for different currents

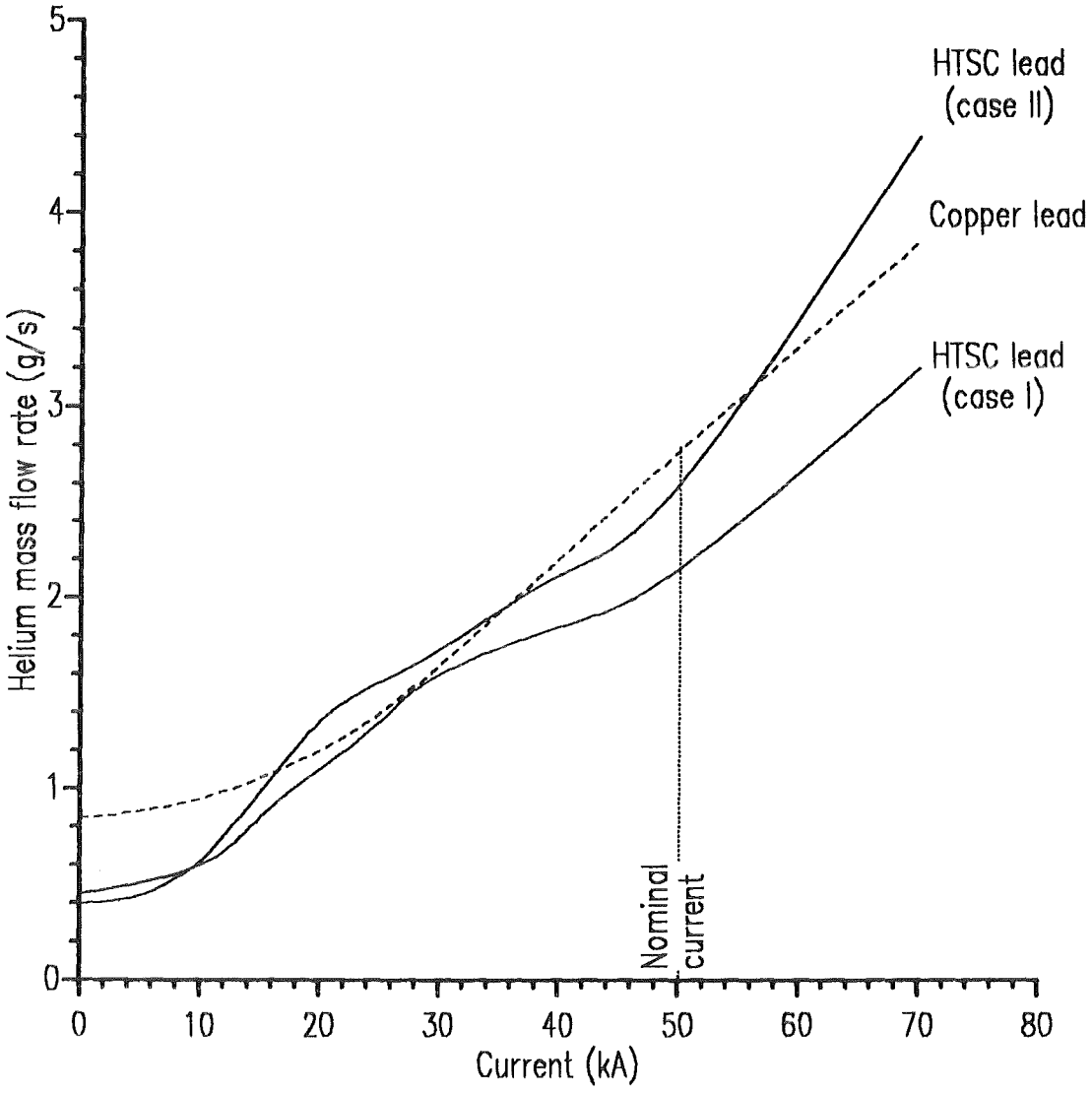

Figure 12. Minimized helium mass flow rate vs current for the HTSC current lead and comparison to the copper lead. The full lines correspond to the HTSC lead (case I and II), the dashed line to the copper lead with Nb_3Sn inserts

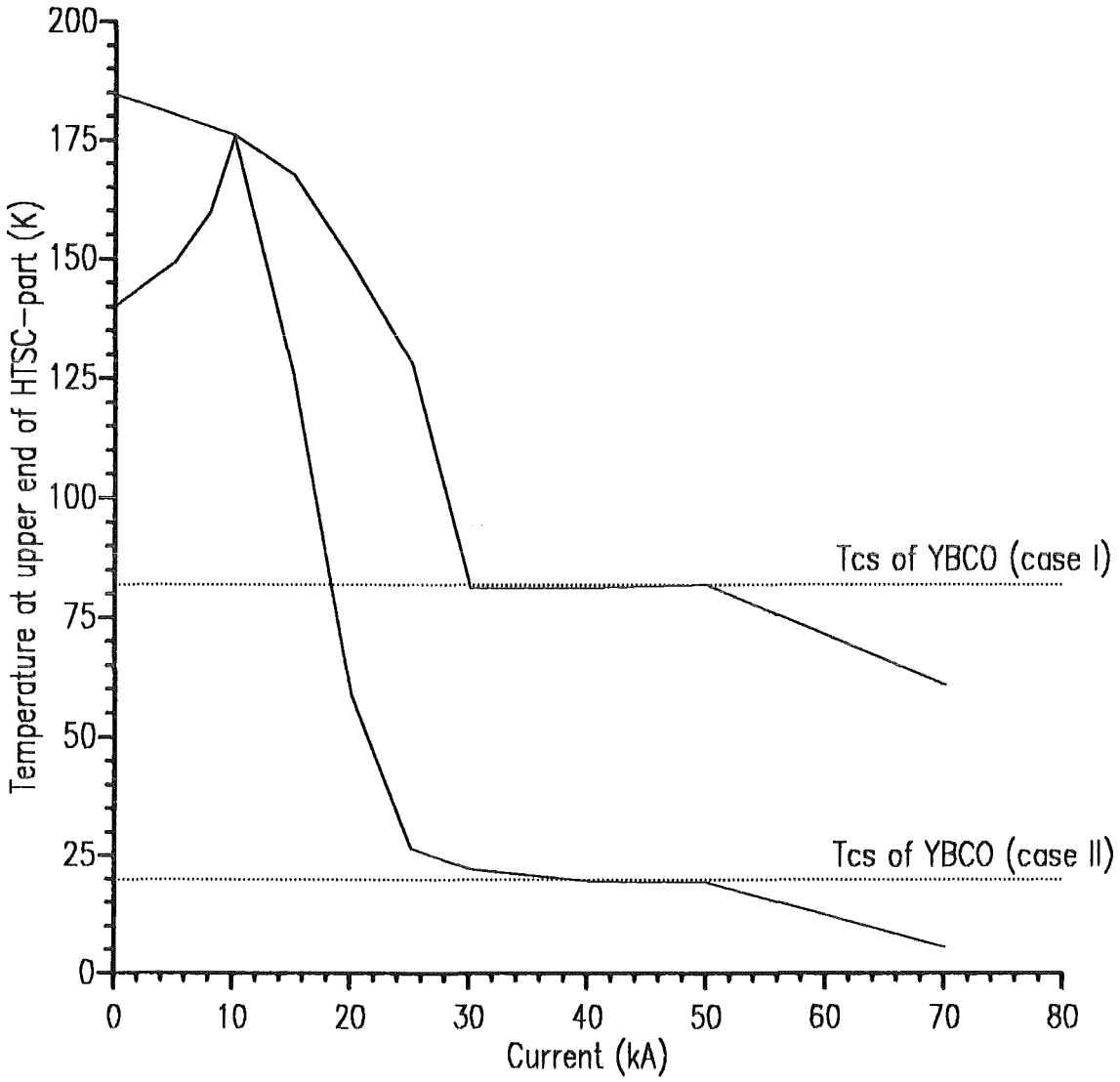

Figure 13. Temperature at the upper end of the HTSC conductor of the current lead vs current

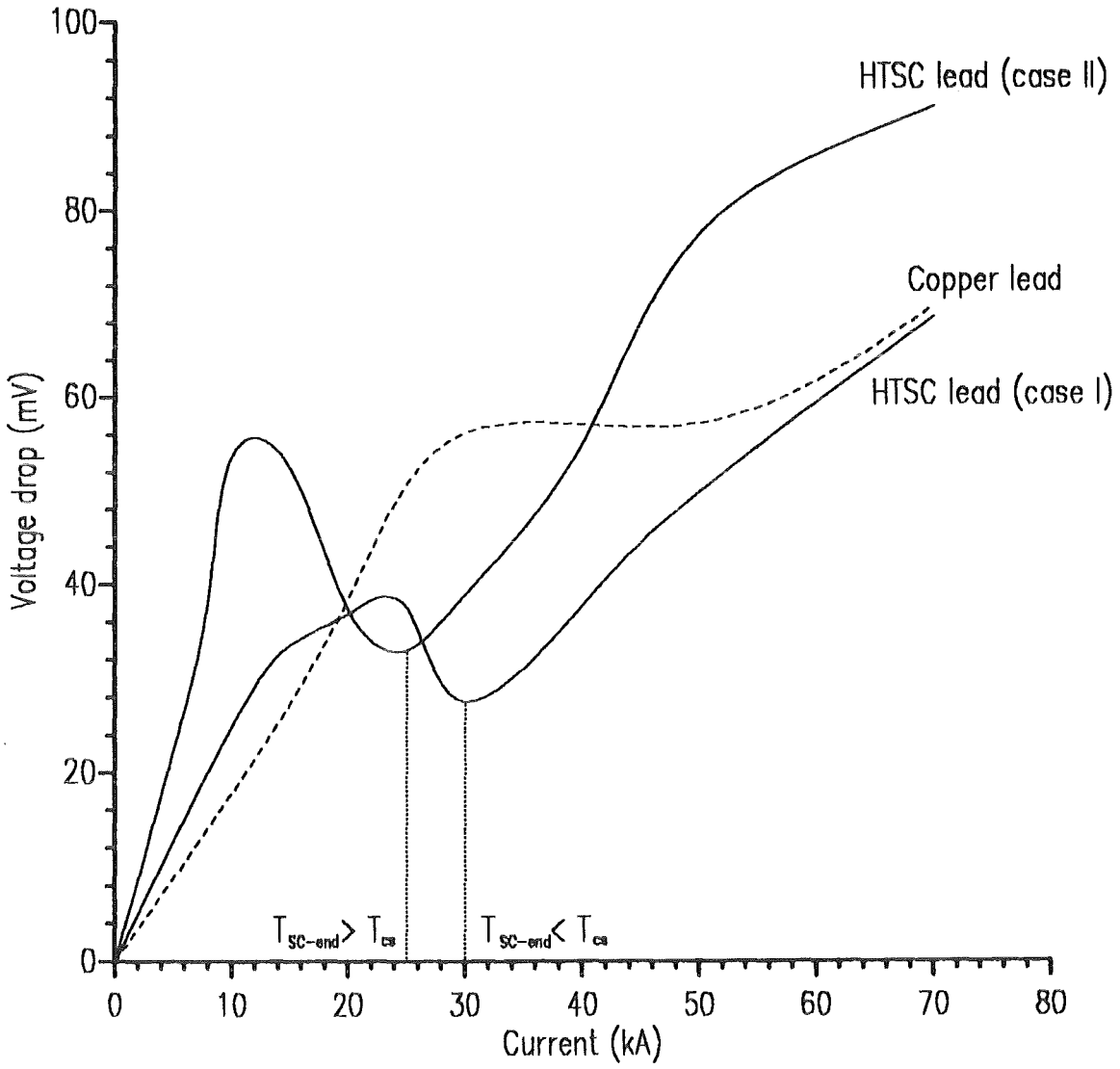

Figure 14. Voltage drop of the current lead vs current. The full lines correspond to the HTSC lead (case I and II), the dashed line to the copper lead with Nb_3Sn inserts

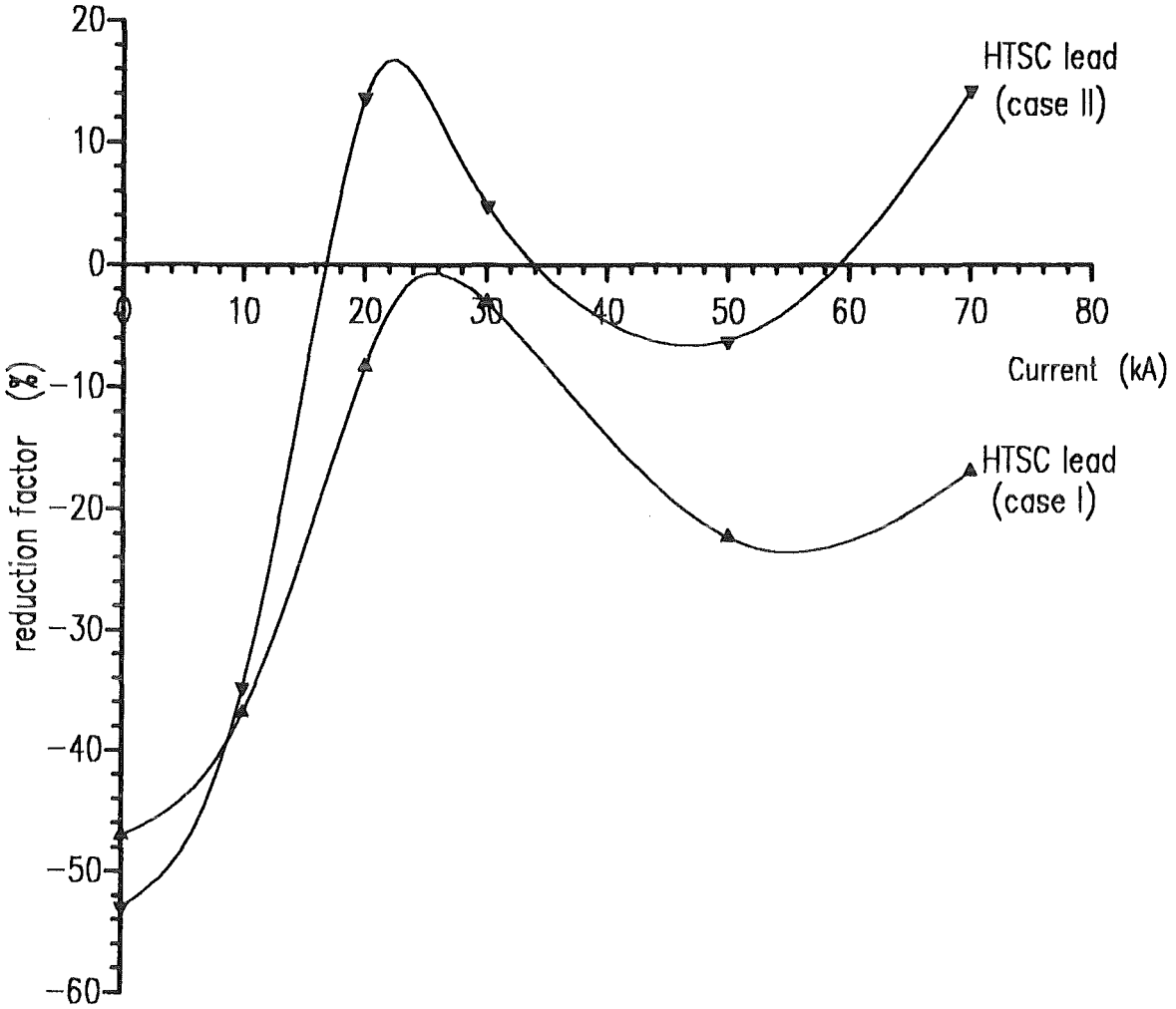

Figure 15. Reduction factor r in % vs current of the HTSC leads and comparison to the copper lead. The full lines correspond to the HTSC lead (case I and II), the dashed line to the copper lead with Nb_3Sn inserts

The results of the steady state load line calculations for the POLO-type copper lead and the HTSC lead of cases I and II are summarized in Table 3 on page 21.

I [kA]	$\dot{m}$ $[\frac{g}{s}]$	ΔU [mV]	Δp [mbar]	Q_{bottom} [W]	T_{cold} [K]	$T_{max,Cu}$ [K]	$T_{top,He}$ [K]	r [%]
POLO-type copper lead								
0	0.85	0.00	98.	0.63	116.2	293.7	293.2	n.a.
10	0.95	17.83	120.	0.36	117.6	293.7	293.2	n.a.
20	1.20	38.50	200.	0.32	131.2	293.9	293.4	n.a.
30	1.65	56.30	346.	0.0	135.3	294.2	293.6	n.a.
50	2.77	57.27	485.	0.0	64.9	293.6	292.4	n.a.
70	3.85	69.85	740.	0.0	36.8	294.0	292.9	n.a.
HTSC lead - case I								
0	0.45	0.00	25.	0.59	184.8	294.3	294.1	-47.1
10	0.65	24.90	45.	0.65	176.3	294.2	294.0	-31.6
15	0.85	33.45	70.	0.0	167.9	294.2	293.9	n.a.
20	1.10	36.87	102.	0.0	149.3	294.0	293.6	-8.3
25	1.35	37.57	134.	0.0	128.3	293.9	293.2	n.a.
30	1.60	27.57	148.	0.0	81.5	293.4	292.4	-3.0
40	1.85	37.91	198.	0.0	80.9	293.7	292.8	n.a.
50	2.16	49.71	276.	0.0	81.3	294.2	293.5	-22.0
70	3.20	68.66	539.	0.0	61.0	294.9	294.7	-16.9
HTSC lead - case II								
0	0.40	0.00	37.	0.62	140.1	294.4	294.2	-52.9
5	0.44	22.25	44.	0.74	149.1	294.4	294.3	n.a
8	0.53	38.60	63.	0.64	159.8	294.5	294.3	n.a
10	0.62	53.80	87.	0.66	175.7	294.6	294.4	-34.7
15	0.98	52.43	157.	0.0	126.3	294.3	294.0	n.a.
20	1.35	37.31	191.	0.0	59.0	293.7	293.0	12.5
25	1.56	33.01	203.	0.0	26.9	293.4	292.5	n.a.
30	1.73	39.07	245.	0.0	22.5	293.5	292.6	4.8
40	2.12	55.22	382.	0.0	19.9	293.9	293.2	n.a.
50	2.60	77.63	641.	0.0	19.4	294.9	294.7	-6.1
70	4.40	91.04	1258.	0.0	5.8	294.7	294.3	14.3

Table 3. Main results of the load line calculations for the POLO-type copper and and for the HTSC leads of cases I and II. Q_{bottom} = heat leakage at low temperature end of the lead, T_{cold} = temperature at the upper end of the supercondcutor carrying part, $T_{max,Cu}$ = maximum temperature in copper conductor, $T_{top,He}$ = helium outlet temperature, n.a. = not applicable

3.0 Loss of helium mass flow

An important feature of a high current carrying current lead is its behaviour in case of loss of helium mass flow. In the study, the leads have been loaded to 50 kA reaching steady state conditions. Afterwards the helium mass flow was stopped, and the temperature distributions voltage drops and heat leakages have been computed at different times while the current stays at 50 kA. In the calculations the heat capacity of the stagnant helium has been included in the energy balance as well as the heat capacity of the copper cooling disks of the heat exchanger. The conductor temperatures at the low temperature end of the leads have been set to the ones of the steady state conditions, i.e. $T_{He,bot} = 4.5$ K, and fixed during the transients.

Figure 16 and Figure 17 show the temperature profiles of the HTSC leads of cases I and II for different times after stopping the helium mass flow. For comparison the temperature profiles of the POLO-type copper lead at different times have been plotted in Figure 18.

In the figures the fundamental distinction between the HTSC and the copper leads is seen which has been described already in the first section of this chapter: the high electrical resistivity and the low thermal conductivity of the HTSC in the normal conducting case leads to a fast rise of the temperature because the Joule heat generated can not be conducted fast to both ends of the heated region. The difference between the HTSC lead of case II to that of case I is the longer copper conductor producing also more heat.

Figure 19 shows the maximum temperature in the HTSC part of the leads of cases I and II as a function of time after stopping the helium mass flow. This figure illustrates the latter fact of a more dramatic increase of the temperature of the lead of case II compared to that of case I. The same behaviour is illustrated in Figure 20 where the voltage drop along the HTSC leads is plotted as a function of time (full lines) and compared to the copper lead (dashed line). The voltage drop related to a maximum temperature in the HTSC part of 700 K is indicated as a full circle.

Figure 21 shows the heat leakage at the low temperature end of the leads as a function of the voltage drop along the leads. The higher voltage drop of the HTSC lead of case II compared to the POLO-type copper lead due to the higher electrical resistivity is clearly seen as well as the fact that the heat leakage of the HTSC lead of case I is negligible even if the maximum temperature of the HTSC part rises upon 700 K. The latter point is indicated as a full circle.

The conclusion is that the HTSC leads are less stable than the POLO-type copper lead. Moreover, the HTSC conductor has to be controlled by a quench detection system based on the temperature or the voltage drop which will initiate a safety discharge of the supercondcuting coil. The time scale will be not so dramatic, i.e. a discharge time constant of 1 min should be large enough not to get into trouble.

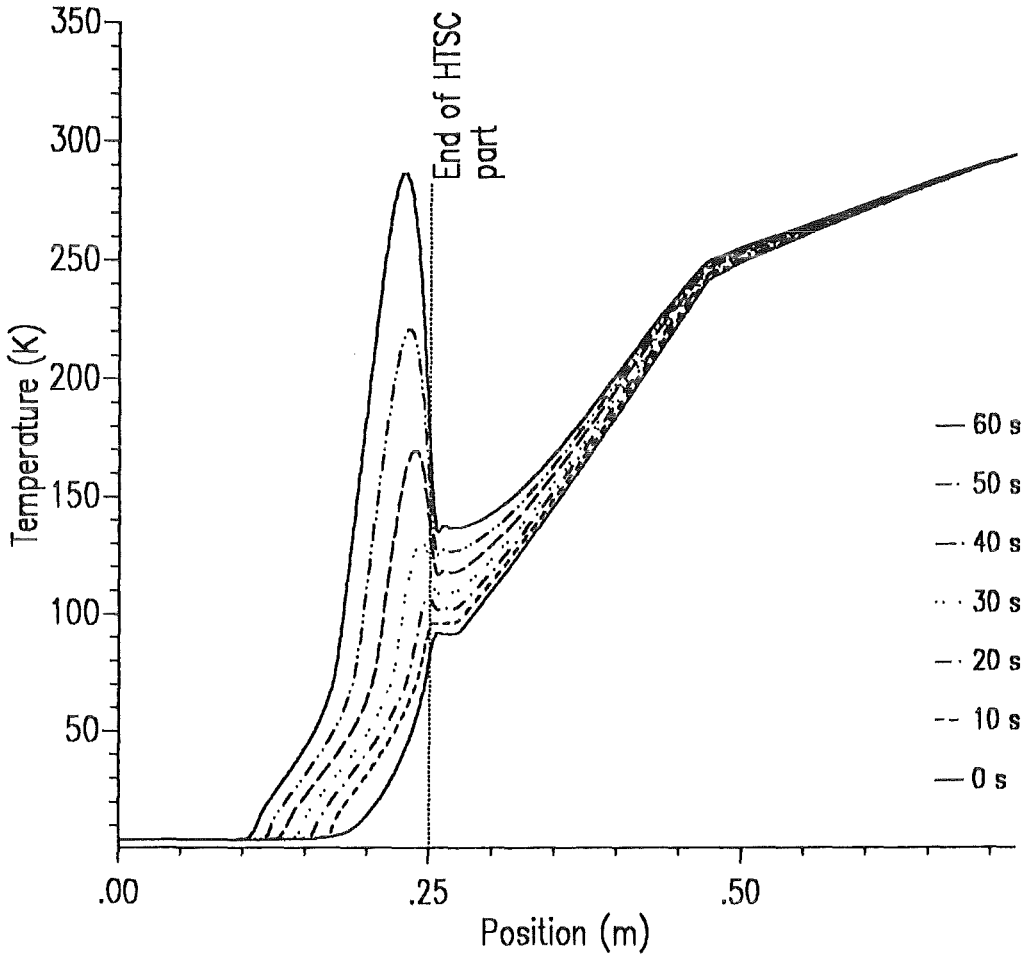

Figure 16. Temperature profile of the HTSC lead (case I) vs position in case of loss of mass flow at 50 kA

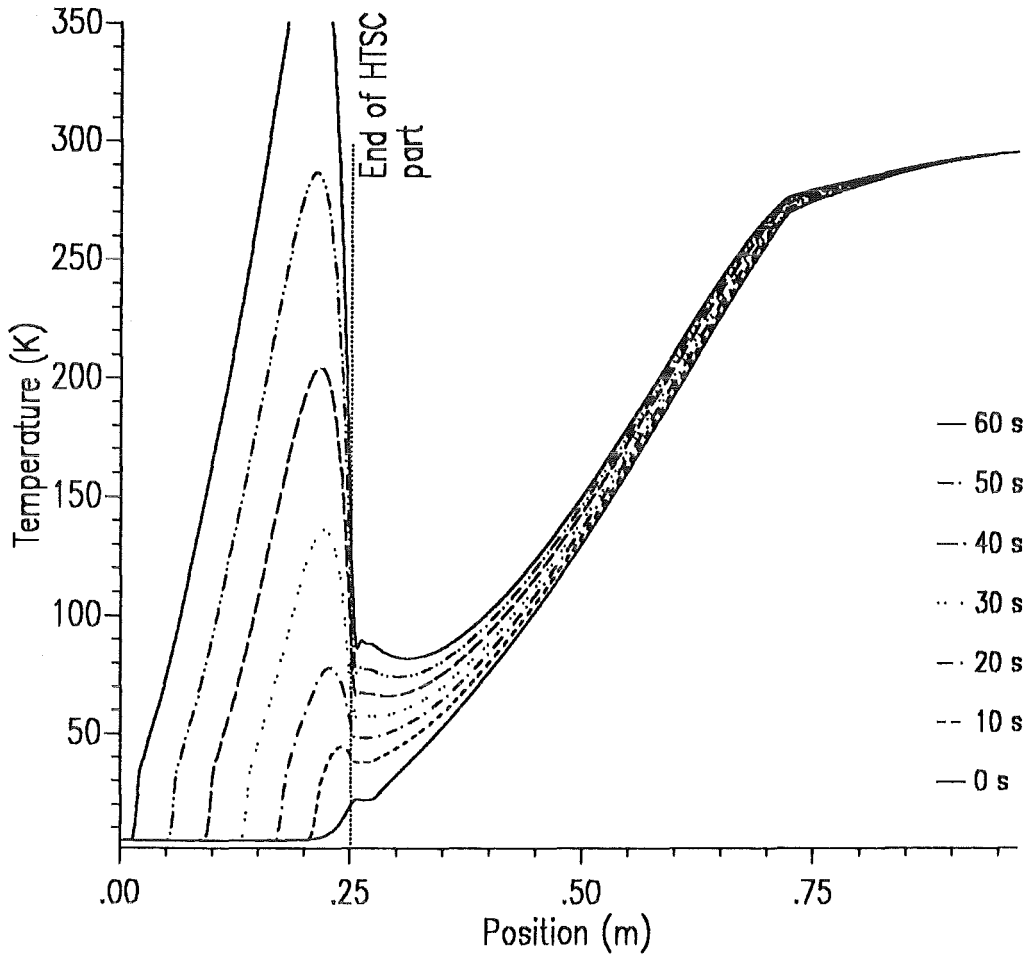

Figure 17. Temperature profile of the HTSC lead (case II) vs position in case of loss of mass flow at 50 kA

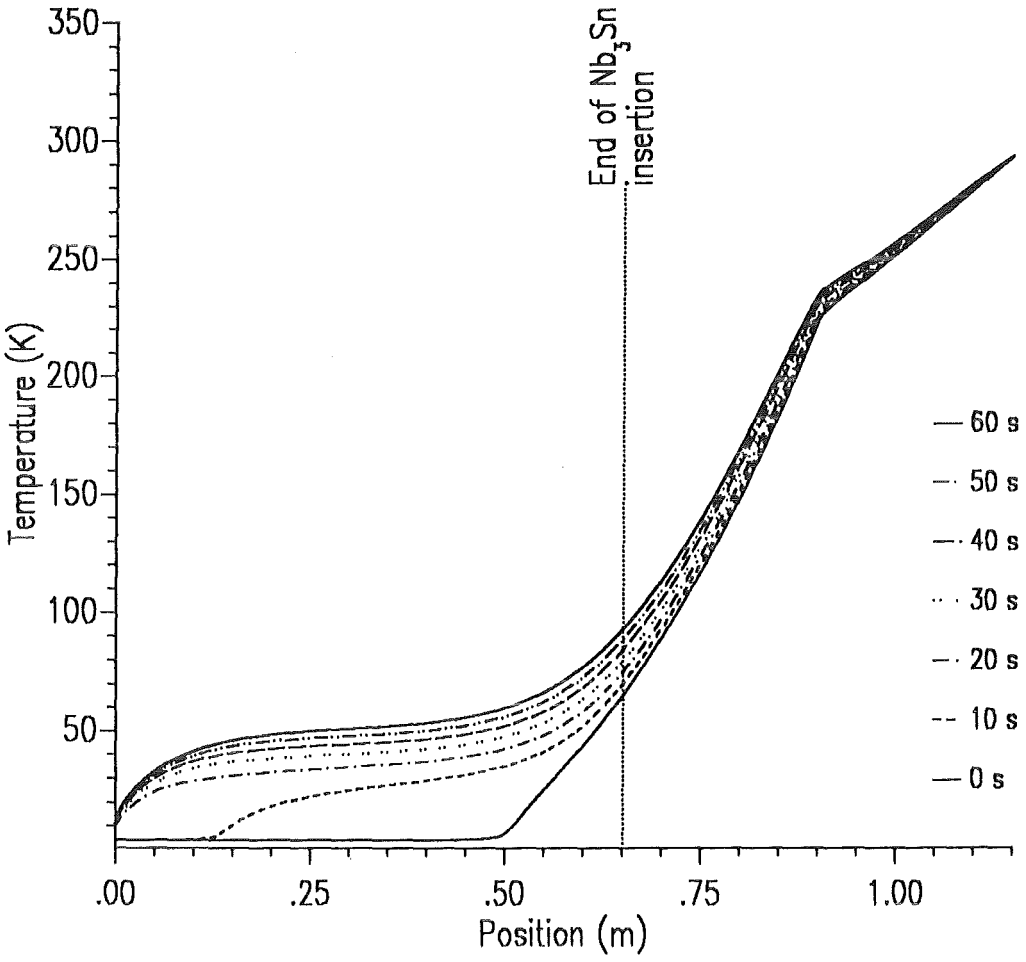

Figure 18. Temperature profile of the copper lead vs position in case of loss of mass flow at 50 kA

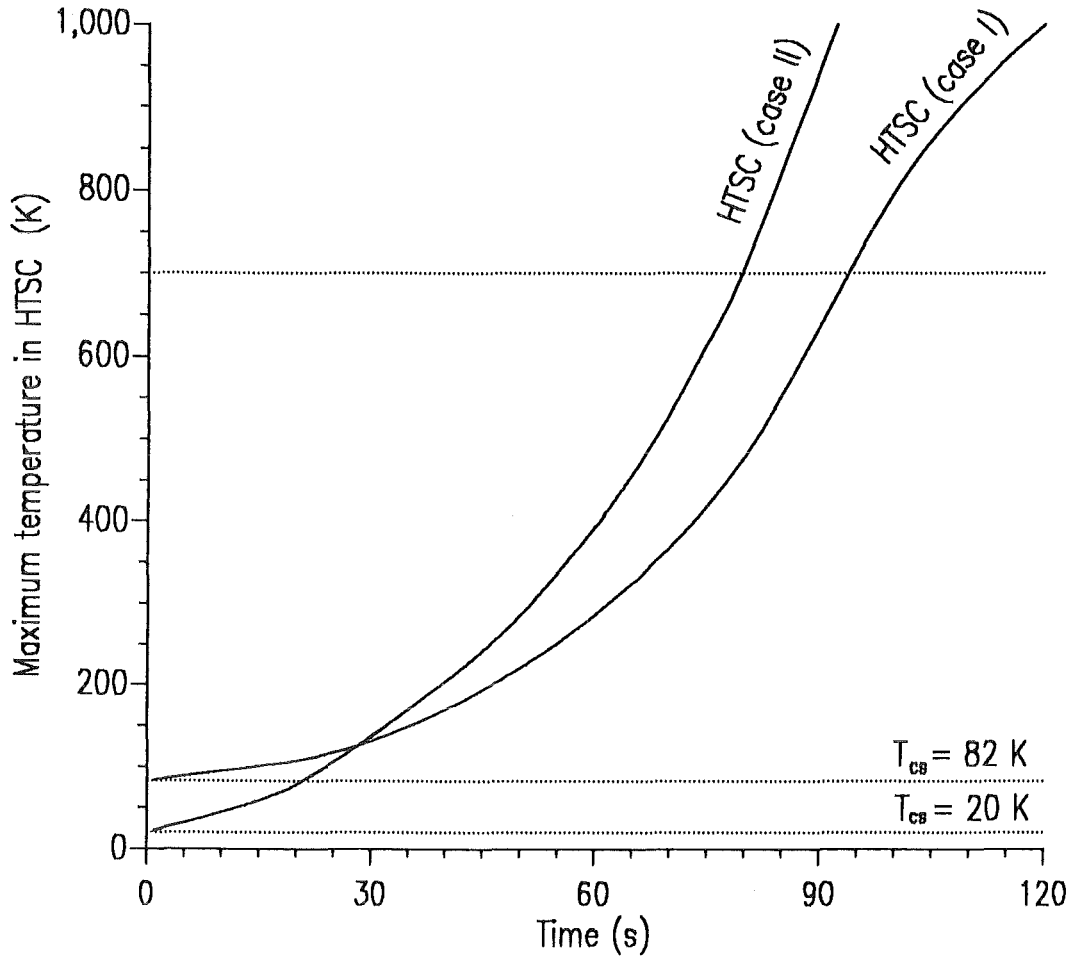

Figure 19. Maximum temperature in the HTSC part of the HTSC leads vs time in case of loss of mass flow at 50 kA

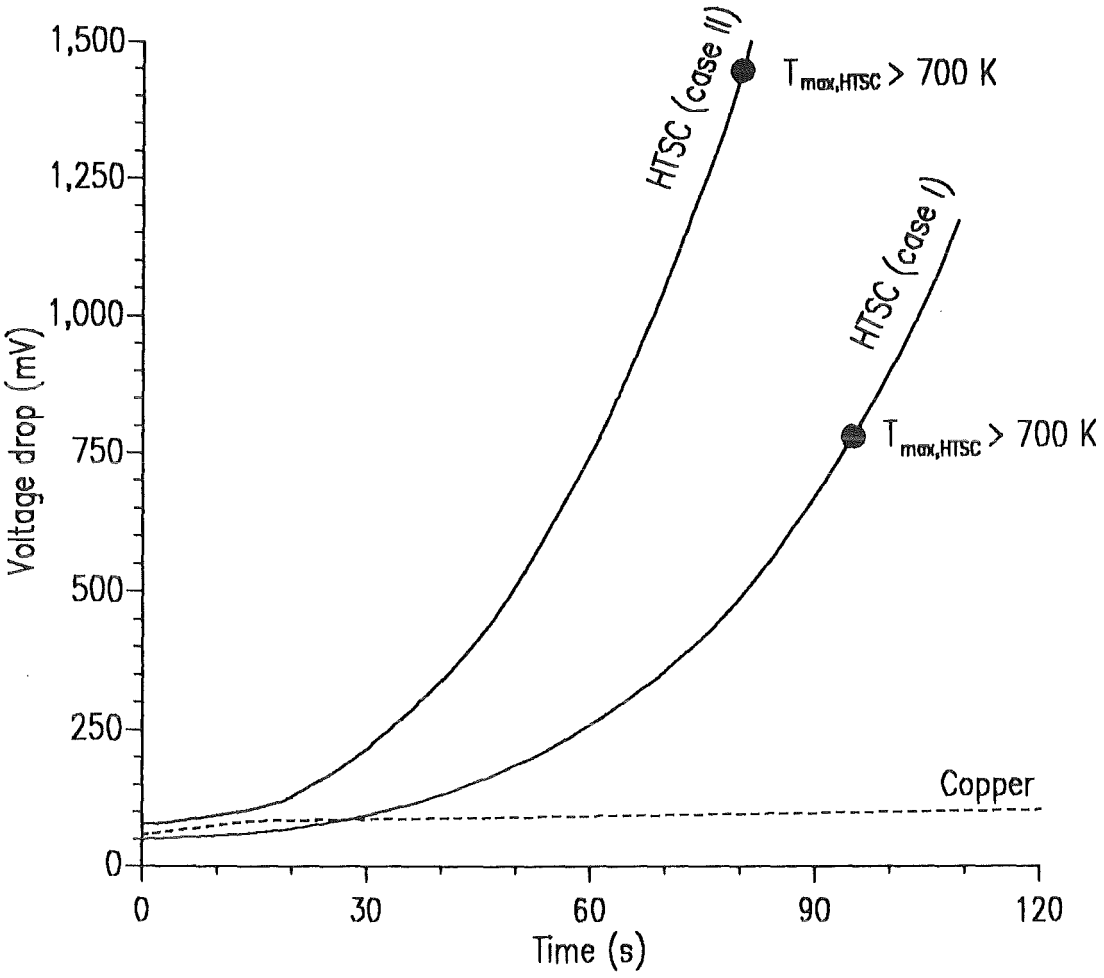

Figure 20. Voltage drop along the current lead vs time of the HTSC leads and the copper lead in case of loss of mass flow at 50 kA. The full lines correspond to the HTSC lead (case I and II), the dashed line to the copper lead with Nb_3Sn insertions. The full circles denote the points where the maximum temperature in the HTSC region exceeds 700 K

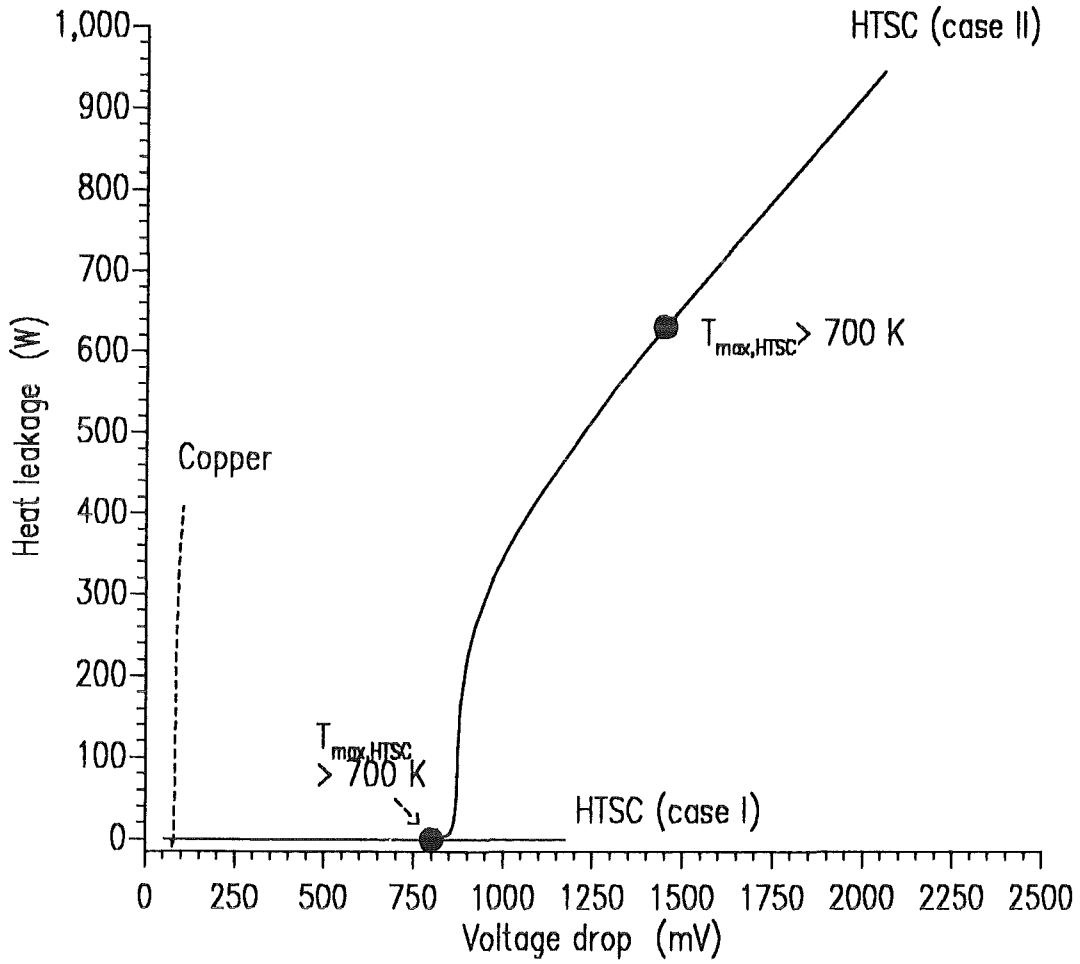

Figure 21. Heat leakage at the low temperature end of the HTSC leads and the copper lead vs voltage drop in case of loss of mass flow at 50 kA. The full lines correspond to the HTSC lead (case I and II), the dashed line to the copper lead with Nb_3Sn insertions. The full circles denote the points where the maximum temperature in the HTSC region exceeds 700 K

4.0 Summary and conclusions

A design of a 50 kA current lead consisting of a HTSC part in the low temperature region and a copper part in the high temperature region has been presented. The steady state behaviour at nominal current, i.e. 50 kA, at stand-by condition, and at 70 kA extended condition has been studied. The transient behaviour in case of loss of mass flow has been investigated as well.

As a result of the requirements given in chapter 2, the following design was chosen:

- HTSC part:
  The total cross section of the HTSC conductor is subdivided in a large number of rectangular rods. The unit size of a HTSC rod is 10 mm x 5 mm, the number of rods is 348, the distance of the rods is 1 mm in both directions. The supercritical helium flows in between. The length of each HTSC rod will be 250 mm.

  Due to the strong dependency of the critical current of the HTSC on the applied magnetic field at 77 K, two designs are made, one with a current sharing temperature of 82 K and a critical temperature of 95 K (design case I), another design with a current sharing temperature of 20 K and a critical temperature of 30 K (design case II). The length of the HTSC conductor is not affected by these two design cases.
- Copper part:
  The copper part consists of a POLO-type heat exchanger, i.e. a central copper conductor (RRR = 6) surrounded by perforated cooling disks for helium cooling. The diameter of the circular conductor will be 70 mm i.e. as for the POLO lead. The cooling disks are made of OFHC copper (RRR = 50) with an outer diameter of 135.7 mm. The length of the copper heat exchanger will be 200 mm for case I, and 450 mm for case II.
- Transition region:
  The adaptation of the HTSC part to the copper part will be done by a 20 mm thick copper disk (RRR = 50) with an outer diameter of 205.7 mm having some cooling holes at well defined locations. A similar adapter piece can be used for the connection of the HTSC part to the magnetic device / superconducting bus bar.

  The HTSC rods which are prepared at both ends with silver contacts will be soldered to the copper disks. The space requirement for the HTSC part lead to the question whether it is possible to solder such a large number of rods.
- Warm end connection to the water-cooled power cables of the power supply:
  This will be done in the same way as already described for the 50 kA current lead proposed for the ITET model coil test in TOSKA [1].

Table 4 summarizes the geometrical numbers of the HTSC current lead design. Figure 22 shows a schematic view of the design case I.

Parameter	Unit	Value	
		HTSC part	Copper part
Heat exchanger type		rectangular rods parallel orientated	central conductor surrounded by perforated copper plates
Length	m	0.25	0.20 (case I) 0.45 (case II)
Cross section of conductor A_{Cu}	cm^2	174.0	38.5
Cooled perimeter of heat exchanger P_{cool}	m	10.44	11.77
Cross section of helium A_{He}	cm^2	159.0	3.86
Inner diameter of cooling disks	mm		70.
Outer diameter of cooling disks	cm		135.7
Transversal distance of cooling disks	mm		2
Disk thickness	mm		1
Hole diameter in cooling disks	mm		0.5
Minimum hole distance in cooling disks	mm		2.5
RRR of cooling disks			50
Rib efficiency of cooling disks		n.a.	function of temperature
Cross sectional dimensions of HTSC rod	mm x mm	10 x 5	
Spacing between HTSC rods in both transverse directions	mm	2	
Number of HTSC rods		348	
Total length of lead	m	0.72 (case I) 0.97 (case II)	
Conductor temperature at upper end of HTSC part	K	< 82 (case I) < 20 (case II)	
Conductor temperature at high-temperature end	K	295	

Table 4. Geometrical quantities of the heat exchanger of the HTSC current lead

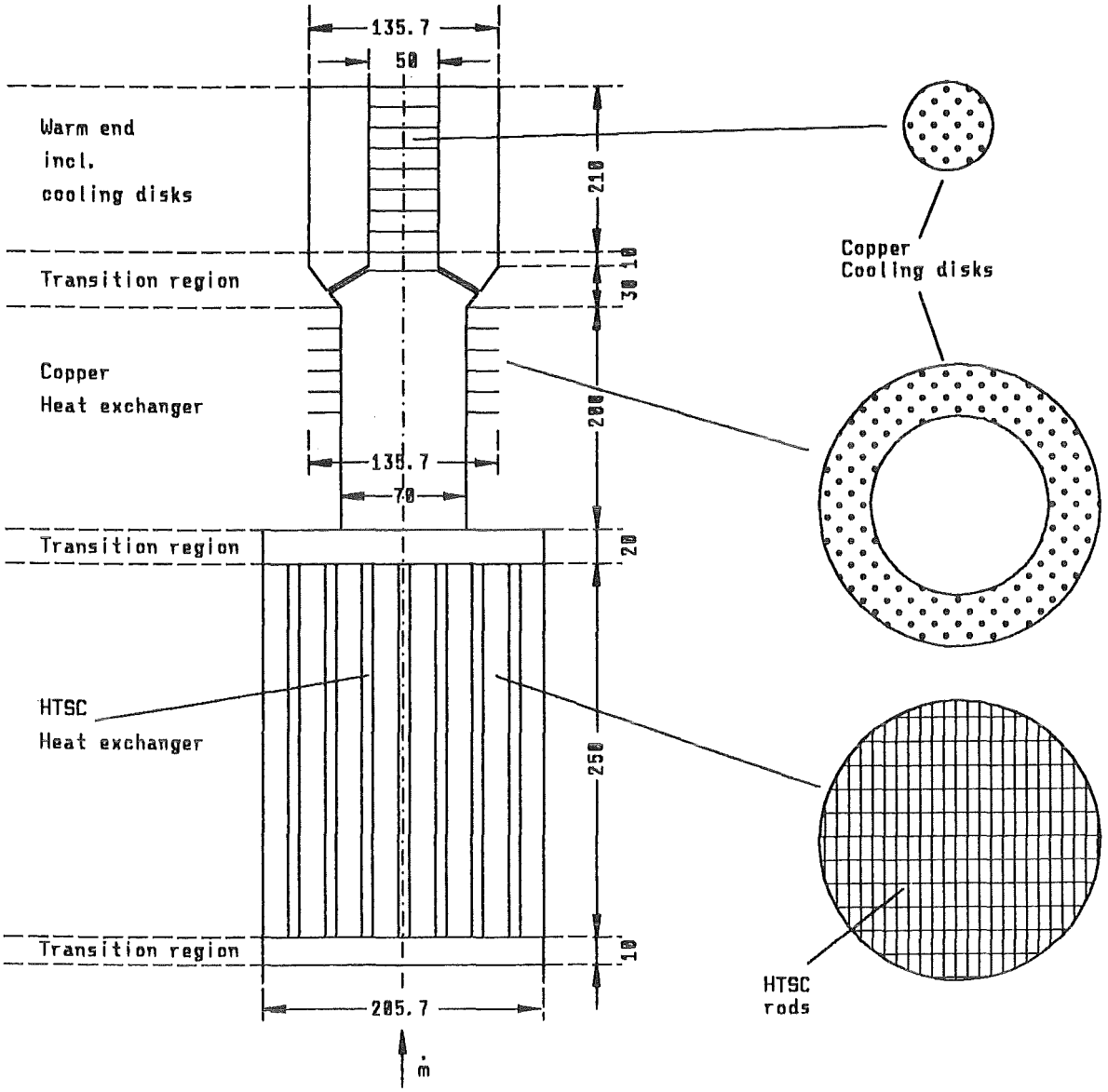

Figure 22. Schematic view of the 50 kA-HTSC-current lead

A comparison was done between the HTSC leads of cases I and II and a POLO-type lead. Table 5 shows the helium mass flow rates normalized to the current for 0 kA and 50 kA. The conclusion is that the reduction of mass flow rate at nominal current is not dramatic as already presented in section 3. Moreover it is the largest at zero current which is not neglegible for an experimental facility. A further reduction could be emphasized using pure BSCCO instead of silver doted YBCO. This is in agreement with results presented by other authors on smaller current leads.

Current	Mass flow rate normalized to current		
	Copper	HTSC case I	HTSC case II
0 kA	0.017 g/(s-kA)	0.009 g/(s-kA)	0.008 g/(s-kA)
50 kA	0.055 g/(s-kA)	0.043 g/(s-kA)	0.052 g/(s-kA)

Table 5. Helium mass flow rates normalized to the current at 0 kA and 50 kA for the HTSC leads and the copper lead

The numbers given above can be used to estimate the margin in cooling power resulting in different power margins for an ITER model coil test in TOSKA. These numbers are given in Table 6. The latter numbers are based on values presented in [3]

Parameter	Value		
	Copper	HTSC case I	HTSC case II
Nominal current	60 kA		
Warm gas flow rate (3 x 60, 2 x 0 kA)	11.94 g/s	8.82 g/s	10.32 g/s
Available refrigeration capacity at 4.5 K	1000 W	1320 W	1200 W
Needed refrigeration capacity at 4.5 K	535 W		
Available margin	465 W	785 W	675 W

Table 6. Cryogenic load of the HTSC leads and comparison to the copper lead for the ITER model coil test in TOSKA

Care has been taken on regarding the transient behaviour of the HTSC leads in case of a loss of mass flow. Here the HTSC conductor will quench, producing the Joule heat which will cause a rise in temperature being much faster than in case of a POLO-type current lead even with Nb_3Sn inserts. This requires a quench detection system for the HTSC part of the lead based either on the temperature at the upper end of the HTSC part or the voltage drop along the HTSC conducting part. After quench detection, the superconducting coil has to be discharged, but the time scale will be in the order of 1 min, i.e. an energy dump should cause no problems.

5.0 References

[1] G. Friesinger, R. Heller, H. Katheder, and G. Zahn, "Numerical study for a 50 kA Current Lead for the NET Model Coil Test in TOSKA-Upgrade", KfK 4947, (1991)

[2] G. Friesinger, R. Heller, W. Herz, M. Irmisch, G. Nöther, L. Schappals, K. Schweikert, L. Siewerdt, M. Süßer, A. Ulbricht, F. Wüchner, G. Zahn, (1992), unpublished

[3] The NET-Team: M.L. Browne, H. Katheder, N. Mitchell, D. Robinson ITP: R. Heller, W. Herz, L. Siewerdt, M. Süßer, F. Spath, A. Ulbricht, F. Wüchner, G. Zahn, (1991), unpublished

[4] D. Eckert, M. Endig, F. Lange, "Gas cooled current leads of variable cross-section for helium cryostats", Cryogenics, (1970), 138-141

[5] G. Claudet, G. Friesinger, R. Heller, U. Jeske, F. Viargues, (1991), unpublished

[6] M.A. Green, "The role of superconductor in reducing the refrigeration needed to cool the leads of a superconducting magnet", Cryogenics, 30, (1990), 679-683

[7] M.A. Hilal, "Optimization of current leads for superconducting systems", IEEE Trans. on Magn., Vol. MAG-13, No. 1, (1977), 690-693

[8] R.K. Thomas, J.R. Purcell and R.W. Boom, "High-current power leads for Tokamak Fusion Reactor Superconducting Magnets", Adv. in Cryog. Eng. Vol. 23, (1977), 219-225

[9] J.R. Hull, "High temperature superconducting current lead for cryogenic apparatus", Cryogenics Vol. 29, (1989), 1116-1123

[10] J.R. Hull, A. Unal, and M.-C. Chyu, "Analysis of self-cooled binary current leads containing high temperature superconductors", Cryogenics Vol. 32, (1992), 822-828

[11] J.L. Wu, J.T. Dederer, S.K. Singh, and J.R. Hull, "High temperature superconducting current leads for fusion magnet systems", 14th Symp. on Fus. Eng., San Diego, (1991)

[12] A. Matrone, G. Rosatelli, and R. Vaccarone, "Current leads with High T_c superconductor bus bars", IEEE Trans. on Magn. Vol. 25 (2), (1989), 1742-1745

[13] J.L. Wu, J.T. Dederer, P.W. Eckels, S.K. Singh, J.R. Hull, R.B. Poeppel, C.A. Youngdahl, J.P. Singh, M.T. Lanagan, and U. Balachandran, "Design and testing of a high temperature superconducting current lead", IEEE Trans. on Magn. Vol. 27 (2,3), (1991), 1861-1865

[14] D.U. Gubser, M.M. Miller, L. Toth, R. Rayne, S. Lawrence, N.McN. Alford, and T.W. Buttons, "Superconducting current leads of YBCO and PB-BSCCO", IEEE Trans. on Magn. Vol. 27 (2,3), (1991), 1854-1857

[15] F. Grivon, A. Leriche, C. Cottevieille, J.C. Kermarrec, A. Petitbon, and A. Fevrier, "YBaCuO current lead for liquid helium temperature applications", IEEE Trans. on Magn. Vol. 27 (2,3), (1991), 1866-1869

[16] O.F. Herrmann, C. Albrecht, J. Bock, C. Cottevieille, S. Elschner, W. Herkert, M-O. Lafon, H. Lauvray, A. Leriche, W. Nick, E. Preisler, H. Salzburger, J-M. Tourre, T. Verhaege, " European project for the development of high T_c current leads", to be published in IEEE Trans. on Magn., (1993)

[17] R.C. Niemann, Y.S. Cha, and J.R. Hull, "Performance measurements of superconducting current leads with low helium boil-off rates", to be published in IEEE Trans. on Magn., (1993)

[18] K. Tasaki, D. Ito, H. Ogiwara, K. Numata, A. Hane, and K. Hoshino, "Development of Oxide Superconducting Current Lead", to be published in IEEE Trans. on Magn., (1993)

[19] K. Ueda, T. Bohno, K. Takita, K. Mukae, T. Uede, I. Itoh, M. Mimura, N. Uno, T. Tanaka, "Design and testing of current leads using bismuth compound superconductor", to be published in IEEE Trans. on Magn., (1993)

[20] J.L. Wu, "Testing of high temperature superconductors for cryogenic current lead applications", to be published in IEEE Trans. on Magn., (1993)

[21] O. Beckman, L. Lundgren, P. Nordblad, L. Sandlund, P. Svedlindh, T. Lundström, and S. Rundquist, "Specific heat and magnetic susceptibility of single phase Y $Ba_2Cu_3O_7$" Physics Letters Vol. 125 No. 8, (1987), 425-428

[22] R. Heller, "Numerical Study of a 50 kA Superconducting Bus for the NET/ITER Model Coil Test in TOSKA-Upgrade", KfK 5008, (1992)

[23] R. Heller, "Numerical calculation of current leads for fusion magnets", KfK 4608, (1989)

[24] R. Heller and C. Rieger, (1992), unpublished